Activation of peroxymonosulfate by biochar-based catalysts and applications in the degradation of organic contaminants: A review

Chenhui Zhao[1], Binbin Shao[1], Ming Yan[1], Zhifeng Liu*, Qinghua Liang, Qingyun He, Ting Wu, Yang Liu, Yuan Pan, Jing Huang, Jiajia Wang, Jie Liang, Lin Tang*

College of Environmental Science and Engineering, Hunan University and Key Laboratory of Environmental Biology and Pollution Control (Hunan University), Ministry of Education, Changsha 410082, P.R. China

* Corresponding authors at:

College of Environmental Science and Engineering, Hunan University and Key Laboratory of Environmental Biology and Pollution Control (Hunan University), Ministry of Education, Changsha 410082, P.R. China

E-mail: zhifengliu@hnu.edu.cn (Z. Liu)

E-mail: tanglin@hnu.edu.cn (L. Tang)

[1] The authors contribute equally to this paper.

Abstract

Sulfate radical-based advanced oxidation processes (SR-AOPs) have received intensively attention due to the ability and adaptability. Biochar-based catalysts have been regarded as the effective catalysts for activating peroxymonosulfate (PMS) to generate sulfate radicals ($SO_4^{\bullet -}$). This article discussed the advance of the PMS activation by biochar-based catalysts. Firstly, the sources and synthesis methods of biochar-based catalysts have been discussed. Secondly, the different activation mechanisms (including radical pathways and non-radical pathways) of pristine biochar, heteroatom doping biochar and biochar composites catalysts for PMS activation are reviewed, respectively, which includes (i) the significant role of persistent radical (PFRs) and the special structures (defects and graphitization) of pristine biochar, (ii) the effects of element doping (especially N atom) and metal species on the biochar catalysts, (iii) the production mechanisms of reactive oxygen species (ROS) and special non-radical mechanism. Thirdly, the influences of PMS and catalysts concentration, temperature, pH, anions and natural organic matter (NOM) on the contaminants degradation process have been presented. Finally, the conclusion and prospects section discussed the challenges and possible future directions for the degradation of contaminants by biochar/PMS systems. This review is expected to provide new ideas for the application of biochar-based catalysts and broaden the ways for the removal of organic contaminants.

Keywords: Biochar-based catalysts; Peroxymonosulfate activation mechanisms; Organic contaminants; Advanced oxidation processes

Contents

1. Introduction.....4

2. Sources and synthesis methods of biochar-based catalysts.....7

2.1 Sources.....7

2.2 Synthesis methods.....10

3. Biochar-based catalysts.....13

3.1 Pristine biochar.....14

3.2 Heteroatom doping biochar.....15

3.3 Biochar composites catalysts.....17

4. Mechanisms of PMS activation by biochar-based catalysts.....18

4.1 Production of ROS: the role of biochar-based catalysts.....19

4.2 Direct electron transfer and surface-bound reactive species.....22

5. Effects of reaction parameters on contaminants degradation.....23

5.1 PMS and catalysts concentration.....24

5.2 Temperature.....26

5.3 pH.....26

5.4 Anions.....28

5.5 NOM.....30

6. Conclusion and prospects.....31

Acknowledgements.....36

References.....37

1. Introduction

Due to the continuous introduction of new chemicals into the environment, the environment pollution has become a challenging multidisciplinary problem in recent years [1-4]. Water pollution caused by refractory organics, especially emerging contaminants (including drugs and personal care products, endocrine disruptors, volatile organic compounds, disinfection by-products, etc.), have caused serious ecological impact [5-9]. Hence, various technologies such as adsorption [10], photocatalytic degradation [11, 12], biological treatment [13-18], enzymatic degradation [19, 20] and advanced oxidation processes (AOPs) [21-25] have been applied to solve the problem of water pollution. Among them, AOPs have received intensively attention because of its great potential in removing organic and inorganic contaminants. The contaminants could be decomposing into low-toxic or non-toxic substances, and even directly mineralized into carbon dioxide (CO_2) and water (H_2O) [26]. However, the oxidants involved in traditional AOPs are hydrogen peroxide (H_2O_2), and the produced radicals are hydroxyl radicals (•OH) [27]. In recent years, sulfate radical-based advanced oxidation processes (SR-AOPs) have gradually emerged due to its unique advantages. Compared with •OH, sulfate radicals ($SO_4^{\bullet-}$) have longer half-life ($SO_4^{\bullet-}$, 30-40 μs, • OH, < 1 μs), higher oxidation potential ($SO_4^{\bullet-}$, E^0 = 2.5-3.1 V, • OH, E^0 = 1.9-2.7 V), stronger selectivity, and are less affected by pH value (pH = 2-8) [28-30]. In addition, persulfate (PS), as a $SO_4^{\bullet-}$ oxidizer, could transport in the solid phase, while H_2O_2 is transport in the liquid phase [31].

$SO_4^{\bullet -}$ are usually produced by PS activation, the PS includes peroxodisulfate (PDS) and peroxymonosulfate (PMS). The physical and chemical properties of PMS and PDS are different: the standard reduction potential of PMS is 1.82 V_{NHE} while PDS is 2.08 V_{NHE}. PMS has an asymmetric structure while PDS has a symmetric structure, and the O-O bond length of PDS (1.497 Å) is longer than that of PMS (1.453 Å) [32]. Different physical and chemical properties between PMS and PDS can lead to differences in the reactivity and activation mechanism. The reactivity of PMS is higher than PDS due to the structural asymmetry, the peroxide bond of PMS has a partial positive charge, while the charge distribution of the peroxide bond of PDS is symmetrical, so non-polar PMS is more vulnerable to nucleophiles [33]. Duan et al. reported that the activation of PMS is dominated by radical pathway, while the activation of PDS is dominated by non-radical pathway involving singlet oxygen ($^1O_2$) and surface activated PDS complexes [34]. However, the cause of this phenomenon (correlation between the different activation mechanisms and physical and chemical properties of PDS and PMS) still needs to be further explored. It may be misleading to draw general conclusions about PS by studying the activation system of single PDS or PMS. So this review only focuses on the activation of PMS. The most commonly used PMS in the laboratory is Oxzone ($2KHSO_5 \cdot KHSO_4 \cdot K_2SO_4$), which a white solid powder. It can be easily dissolved in water and the solubility is greater than 250 g/L [35].

PMS can be activated by many methods, including energy activation (e.g., heat, UV light, ultrasound, and microwaves), transition metal activation (e.g., Co, Fe, Cu,

Mn) and nonmetal carbon activation (e.g., carbon nanotubes, activated carbon, nanodiamonds and graphene, etc.) [36-41]. However, the PMS activation by energy needs continuous energy supply, resulting in a large amount of energy loss and the metal-based activation easily leads to toxic metals exudation and causes secondary pollution. Compared with metal-based catalysts, nonmetal carbon catalysts have the advantages of less pollution and good thermal stability [42]. Dikdim et al. suggested that PMS could improve the degradation of atrazine by activated carbon [43]. Wang et al. indicated that the N-doped graphene (NRGO) could act as the PMS activator and promote the degradation of sulfamethoxazole (SMX) [44]. However, most of the raw materials used to prepare these nonmetal carbon catalysts are expensive, and the preparation process of the catalysts is complicated [26, 45]. From the perspective of application, it's an urgent task to search carbon materials with simple preparation process, environmental friendliness and low cost.

Biomass, such as rice straw [46], wood chips [47], potato waste residue [48], sewage sludge [49], and cotton [50], have been regarded as important precursors for the synthesis of biochar-based catalysts with easy accessibility and sustainable development requirements. Biomass has rich functional groups and good porous structure, which provides natural advantages for the preparation of biochar-based catalysts [51]. Biochar-based catalysts have the advantages of wide sources and simple preparation [52, 53]. In recent years, synthesized highly efficient catalysts which come from waste biomass to activate PMS for organic contaminants degradation have been widely studied [46, 54-56] and the number of research papers

continues to increase (Fig. 1). However, there are no articles reviewing the advance of biochar-based catalysts to activate PMS for organic contaminants degradation.

Consequently, this article reviewed the research progress of various biochar-based catalysts made from different biomass to activate PMS in recent years. The various mechanisms of PMS activation by pristine biochar, heteroatom doping biochar and biochar composites catalysts were reviewed and discussed in detail. Additionally, the activated PMS can be applied in the contaminants degradation and the effects in terms of (i) PMS and catalysts concentration, (ii) temperature, (iii) pH, (iv) anions and (v) natural organic matter (NOM) were analyzed. This article provided a deep comprehension of the mechanisms of biochar-based catalysts to active PMS and summarized the application of PMS for the degradation of organic contaminants.

2. Sources and synthesis methods of biochar-based catalysts

2.1 Sources

In generally, the properties of materials determine their functions, their composition and structure determine their properties. Biomass has evolved different microstructures due to its different functions. Biochar prepared from different biomass will inherit the excellent structure of its precursor, and then showed discrepant characteristics. For example, biochar prepared from bagasse has better pore structure and larger specific surface area than biochar prepared from straw [57, 58]. Human hair-derived biochar not only has large surface area (> 2000 m^2/g), but also forms natural N and S co-doped biochar without add additional N and S sources [59]. The

selection of biochar precursors has an important effect on its catalytic performance. Food waste pristine biochar was reported to efficient activate PMS to degrade azo dye [60], while the myriophyllum aquaticum pristine biochar shows poor activity towards PMS activation [61]. Oh et al. pointed out that the percentage of graphitic N (could be the active site to active PMS) in the biochar various with the choice of waste biomass but structure defects and sp^2-hybridized carbon are not affected by precursors [62]. However, there are many studies concentrate on a single precursor, and there is a lack of systematic comparison between different sources of biochar. How to select the appropriate biomass according to the actual application requirements of biochar is also a problem that should be paid attention to in the future.

Lignocellulosic waste, as a ubiquitous natural resource, consists of cellulose, lignin, and hemicellulose. The composition of lignocellulose varies with the biomass but does not affect the formation of biochar, and the heat treatment will decompose the surface structure of the biomass and carbonize it into porous biochar [63]. The activity and production of biochar is affected by the composition of lignocellulose. Meng et al. pointed out that when the ratio of cellulose in biomass is higher than that of lignin, the activation of PMS will be promoted [64]. Nidheesh et al. suggested that increase the lignin content of biomass would promote the carbonization and increase the production of biochar [65]. Besides this, the analysis of the relationship between lignocellulose composition and catalytic activity of biochar is still relatively limited. Researchers have obtained some fascinating biochar-based catalytic materials to active PMS by pyrolyzing different lignocellulose waste, such as fruit skin,

agricultural waste, wood and waste coffee grounds. Besides lignocellulose biomass, several non-lignocellulose wastes such as sewage sludge, household garbage (food waste and human hair) are applied in the preparation of biochar and the activation of PMS (Table 1). At present, the biomass that has been studied and applied to activate PMS for the degradation of organic contaminants is still limited. Plant-based biochar derived from wood and agricultural waste has been widely used to activate PMS, but there are almost no PMS activators derived from animal manure and litter. Fig. 2 showed the sources of various biochar-based catalysts used in PMS activation and the research gap between plant-based waste and animal-based waste.

Most of the biomass used to activate PMS is the wastes generated in industry, agriculture and daily life that directly discarded or difficult to dispose. For example, using sludge as the precursor of biochar not only effectively treats sludge, but also provides a new idea for the preparation of biochar. Converting carbon-rich agricultural wastes into biochar is a promising option. The wheat straw, maize stalk, rice hull and corncob are pyrolyzed to prepare biochar with large specific surface area, rich oxygen-containing functional groups and stable structure [66]. The actual application potential is often closely related to the processing cost. The cost of biochar produced by rapid pyrolysis is about $560 per ton [67]. Compared with dry wastes such as agricultural wastes and wood (moisture content < 30%), wet wastes such as animal manure and litter and sewage sludge (moisture content > 30%) have higher moisture content and thus require more heat and time [68]. Therefore, biomass with low moisture content has higher economic feasibility.

2.2 Synthesis methods

At present, the preparation methods of biochar include pyrolysis (300-900 ℃) [69], gasification (> 700 ℃) [70, 71] and hydrothermal carbonization (180-250 ℃) [72-74]. However, the preparation methods of biochar for catalytic degradation are not significantly different [75]. The most conventional method to preparing biochar catalysts for catalytic degradation is pyrolysis, and the gasification and hydrothermal carbonization processes even have not confirmed the circumscription of biochar. Pyrolysis is usually carried out under oxygen-limited conditions at 300 to 900 ℃ [76], and the solid, liquid and gas products are formed together, the solid content is called biochar. The synthesis methods of pristine biochar, heteroatom doping biochar and biochar composites catalysts will be discussed in detail in the next paragraph.

The preparation of the pristine biochar is very simple. The biomass is washed, crushed, sieved and direct pyrolyzed in a tube furnace or a muffle furnace. Some scholars wash the obtained product with HCl and KOH to remove residual inorganic impurities and silicate [77]. For the preparation of heteroatom doping biochar, it can be divided into one-pot synthesis method and post-treatment method. The one-pot synthesis method is to mix the chemical reagents containing heteroatoms with the biomass for pyrolysis. Oh et al. prepared N-doped biochar (NBC) using an easy-to-operate pyrolysis process [62] (Fig. 3A). The introduction of N heteroatom is usually achieved by adding urea. Zaeni et al. demonstrated that increasing the initial urea concentration, the formation of graphitic N could be promoted [78]. Besides urea, thiourea, melamine and dicyandiamide can also be used as N atom introduction

reagents. Xu et al. explored the influence of four different N precursors (thiourea, urea, melamine and dicyandiamide) on PMS activation, and found that N-doped biochar prepared by dicyandiamide as N precursors had the best activation effect on PMS [79]. The post-treatment method refers to mixing the prepared biochar sample with chemical reagents and then pyrolyzing them again. Wang et al. prepared sulfurized biochar derived from sewage sludge (SSB) using the method of post-treatment [80].

As for biochar composites catalysts, the preparation processes are relatively diversified but can also be divided into one-pot synthesis method and post-treatment method. Tian et al. prepared Co@C core-shell nanoparticles containing N and S porous biochar catalysts (Co-NS-PCs) using an easy-to-operate one-pot pyrolysis strategy [81]. Du et al. synthesized the S-Co_3O_4 assembled N doped biochar catalyst (Co-S@NC) using the method of one-step pyrolysis [82]. The preparation processes and formation mechanisms of Co-NS-PCs and Co-S@NC are shown in Fig. 3B and Fig. 3C. Co-NS-PCs were synthesized by mixing the wheat flour, sodium bicarbonate cysteine and cobalt nitrate hexahydrate, and pyrolying the dried mixture. Co-S@NC is obtained by pyrolysis the mixture of sulfate saturated biosorbent and cobalt(II) acetate. Li et al. first prepared the pristine biochar called C400, then mixed C400 and $KHCO_3$ for the second calcination to obtain C800. The dried $Co(NO_3)_2 \cdot 6H_2O$, $Fe(NO_3)_3 \cdot 9H_2O$ and C800 mixture was calcined for the third time to obtain the biochar supported $CoFe_2O_4$ nanocomposite (post-treatment method) [83]. However, the difference and connection of biochar-based catalysts synthesized by one-step synthesis method and post-treatment method, and their different properties for PMS activation still need to

be further explored.

During the pyrolysis process, operating parameters such as pyrolysis temperature, reaction residence time, and pyrolysis atmosphere play important role in the formation of biochar [84]. These operating parameters not only affect the surface properties, but also affect the yield of biochar. Pyrolysis temperature has a great effect on the distribution, composition, yield and calorific value of pyrolysis gas. The different pyrolysis temperature has great influence on chemical and physical properties of biochar, which could then affect the reactivity of biochar-based catalysts [85]. Da et al. pointed out that the porosity and specific surface area of biochar would increase with the increase of pyrolysis temperature [86]. In addition, the increase of pyrolysis temperature would cause the conversion of sp^3-hybrid carbon, resulting in the collapse of the carbon skeleton and increasing the defect structure of biochar so as to increasing the potential for PMS activation. Yu et al. showed that the pyrolysis temperature could not only change the carbon configuration, transform sp^3-hybrid carbon to sp^2-hybrid carbon, but also induce the formation of graded porous carbon [87]. Wang et al. prepared sludge-derived biochar (SBC), compared with the preparation temperature of 700 °C, the catalytic activity of biochar at 600 °C was even decreased by 20%, which might be due to the increase in amorphous carbon content and the decrease in specific surface area of biochar [88]. In addition, in the N-doped biochar/PMS system, the proportion of graphitized N would increase with the rise of pyrolysis temperature. This was because the thermal stability of graphitic N was stronger than that of pyridinic N and pyrrolic N. Pyridine N and pyrrolic N had a

tendency to convert to graphitic N during the pyrolysis process [89].

The reaction residence time will affect the carbonization degree and yield of biochar [90]. It is worth noting that the pyrolysis of biomass usually takes place in N_2 atmosphere. Some recent studies have reported that the use of CO_2 instead of N_2 as the reaction medium can increase the production of natural gas and make the synthesized biochar have better surface properties [91, 92]. Kwon et al. and heidic et al. mentioned in their research that the use of CO_2 as a pyrolysis reaction medium can significantly increase the porosity of biochar [93, 94]. It is well known that the yield and characteristics of biochar are affected by the operating parameters of the pyrolysis process. However, the relationship between operating parameters and the final product seems to be lacking.

3. Biochar-based catalysts

Many researchers have demonstrated that biochar-based catalysts could activate PMS for the degradation of organic contaminants [95, 96]. The biochar-based catalysts used for PMS activation can be divided into pristine biochar, heteroatom doping biochar and biochar composites catalysts. This section discussed the structures and groups associated with PMS activation (active sites) come from three types of biochar-based catalysts, such as persistent free radicals (PFRs), graphitization structures and defect structures, N species (graphitic N, pyridinic N and pyrrolic N) and variable metals (Fig.4).

3.1 Pristine biochar

At present, the researches on activation of PMS by biochar-based catalysts are still in its infancy, and there are not many studies on pristine biochar. This may be due to the limited active sites and catalytic performance of the pristine biochar. However, some scholars still obtained the pristine biochar catalysts with excellent catalytic performance through pyrolysis of biomass [60, 97]. The PFRs and special structures (defect structures and graphitized structures) in the pristine biochar catalysts play an important role in the PMS activation process.

The pristine biochar here refers to the products produced by the pyrolysis of biomass at a certain temperature without adding any compound. Incomplete pyrolysis of biomass will produce PFRs, which the half-life varies from several hours to several days. High temperature calcination (above 700 °C) will decompose most of the PFRs, but some graphitized carbon structures will appear at the same time. PFRs are the key factors affecting the activation ability of biochar [98-100]. Recently, the role of PFRs existed in biochar on the activation of PMS has attracted the attention of some scholars [58, 101]. Numerous studies have reported that PFRs could be used as electron shuttle agents who are beneficial for the mediate electron transfer reactions [102, 103]. Fang et al. proposed that the PFRs could be the redox centers to decompose PDS and elaborated the production mechanisms of PFRs and reactive oxygen species (ROS) in detail [98]. However, in the biochar/PMS system, there is still a lack of reliable researches on the mechanism of PMS activation related to PFRs.

Besides PFRs, structural defects such as edges and disorder in biochar are very

favorable for catalytic degradation. Da et al. studied that the key factor for biochar to activate PMS so as to eliminate 1,4-dioxane was the defect structures rather than the PFRs [86]. They can not only increase the density of active sites by carrying active redox pairs [104, 105], but also serve as active sites for ROS [106]. However, it is worth noting that excessive structural defects will reduce the mechanical strength and durability of biochar, which will affect the catalytic performance of biochar. What' more, the catalytic performance of biochar is closely related to the degree of graphitization [107]. Graphitized structures can not only induce direct electron transfer between contaminants and PMS bridged by the graphitized structures but also promote electron transfer by increasing the charge density of C atoms [83]. What's more, the graphitized structures could stabilize radicals and electrons, thereby increasing the efficiency of active radical in degrading contaminants [108].

3.2 Heteroatom doping biochar

Despite the great diversity in the composition and structure of biochar from different sources, almost all pristine biochar have defects such as limited function and poor anti-interference ability, resulting in limited catalytic capacity [109]. Chemical modification can effectively overcome the above-mentioned shortcomings and break the limitations of the pristine biochar in removing contaminants in the catalytic fields [110-112]. Heteroatom doping is an important modification method. In the past few decades, researchers have tried to synthesize functional catalysts with specific characteristics and enhanced performance by introducing heteroatoms [113, 114]. The

addition of non-metallic heteroatoms into catalytic materials can not only introduce surface defects and change the intrinsic characteristics of biochar catalysts, such as specific surface area and pore diameter, but also increase the amount of Lewis acid sites, thus expanding the active sites [115]. The doping of heteroatoms can significantly strengthen the electron shuttle ability of the catalysts [116]. In the metal-free catalytic systems (except biochar catalysts), the doping of single N, single S, single B and multiple doping (such as N, P-carbon, P, S-carbon, N, S, P-carbon and N, P, S, B-carbon) have been widely studied [115, 117-120]. However, in the biochar/PMS system, the types of doped heteroatoms are still very single, most of which are concentrated on N atoms, and there are small amount of researches focuses on S atoms [80].

The doping of N can significantly enhance the catalytic efficiency of biochar materials during the activation of PMS [50, 121, 122]. Doping N atoms can not only promote the surface adsorption of PMS by increasing the basicity of biochar, but also promote the electron transfer reaction between biochar and PMS by activate the adjacent sp^2-hybrid carbon [123]. The compositions of N species in N-doped biochar were confirmed by the XPS spectra analysis. The N species include graphitic N, pyridinic N and pyrrolic N. Compared with pyridinic N and pyrrolic N, there are more reports about the graphitic N. Graphitic N can be the active site to activate PMS to generate ROS, and it can also be used as adsorption site to adsorb PMS to promote the direct electron transfer between PMS and contaminants [124]. Some scholars also pointed out that pyridinic N and pyrrolic N are also redox active species that are

beneficial to the activation of PMS [89, 125]. Pyridinic N located in the edge of catalysts can play the role of Lewis basic site to induce the redox process [126, 127]. However, as the main active site, the graphitic N would convert into pyridinic N and the reaction was irreversible in the catalytic process, and the pyridinic N and pyrrolic N would be rapidly decomposed (have the cannibalistic reactions with ROS) under highly-oxidizing environment [128]. This phenomenon can be used to explain why the durability of N-doped biochar active sites found by many studies is poor [129].

S atom is similar to N atom that has a unique electronic structure (the outermost p orbital), but its electronegativity is lower. Wang et al. firstly prepared a single S-doped biochar and revealed the unique role of S-doping in the activation of PMS [80]. The zigzag edge S can greatly disturb the electron distribution in the pristine biochar structure, and cooperate with the inherent graphitic N/pyridinic N to create more Lewis acid and basic sites. In addition, S atoms can be used as electron acceptors to accept electrons from PMS to produce $^1O_2$ [82]. It is worth mentioning that compared with single N and S doping, dual N and S doped biochar has higher catalytic activity. This may be due to the synergistic effect of N and S co-doping, which cause the reconstruction of charge density and the spin state of C [130-132].

3.3 Biochar composites catalysts

Besides the heteroatom doping, preparing biochar composites catalysts is another important biochar modification method. The use of biochar-based catalysts to activate PMS to remove contaminants in water has the dual advantages of carbon

sequestration and water pollution control [133]. In recent years, researchers have prepared many biochar composites catalysts with good catalytic performance, such as MnOx-N-biochar composites catalysts, Fe_3O_4 porous biochar composites, graphitized hierarchical porous biochar and $MnFe_2O_4$ magnetic composites catalysts, magnetic nitrogen doped biochar supported $CoFe_2O_4$ composite, Co_9S_8 and CoO encapsulated N and S co-doped biochar [134]. The substances composited with biochar are usually metals with variable valence states such as Co, Fe and Mn, because the valence conversion between metals can induce redox reactions and increase the pathway of ROS production. Constructing metal compound and heteroatoms (N and S) co-composite biochar catalysts is a good idea, which can greatly increase the active sites and break the inert structure of the pristine biochar.

For metal-based catalysts, toxic metal leakage has always been an important factor limiting its practical application. Heterogeneous magnetic catalysts such as MFe_2O_4 (M = Co, Cu, Mn) can alleviate this problem. In the biochar composites catalysts/PMS system, the biochar loaded MFe_2O_4 composites not only solves the problem of toxic metal leakage and the easy agglomeration of MFe_2O_4, but also solves the problem of difficult separation of biochar catalysts due to the presence of magnetic metals (especially Fe) [135, 136].

4. Mechanisms of PMS activation by biochar-based catalysts

The activation mechanism of PMS includes radical mechanism and non-radical mechanism. The radical mechanism is to activate PMS through the active sites on the surface of catalysts (such as defective structure, C=O, sp^2-hybridized carbon, metal

species, etc.) to produce $SO_4^{\bullet -}$ and •OH, so as to achieve the degradation of contaminants. The non-radical mechanism is to produce singlet oxygen ($^1O_2$) as the active species. In addition, a special non-radical activation mechanism, that no ROS are produced, just according to surface electron transfer (contaminants, catalysts, PMS as electron donors, electron shuttles and electron acceptors, respectively) or surface-bound reactive species [137, 138]. In this section, the mechanisms of PMS activation by biochar-based catalysts are discussed in detail.

4.1 Production of ROS: the role of biochar-based catalysts

In the current literatures, SR-AOPs are not limited to $SO_4^{\bullet -}$, but include ROS such as •OH, $^1O_2$, and non-radical pathways without the participation of radicals [33]. Different systems have different conclusions about which ROS plays a leading role. Sun et al. pointed out that when using the N-functionalized sludge carbon (NSC) to active PMS, both non-radical and radical ($SO_4^{\bullet -}$ and •OH) mechanisms existed simultaneously, but $^1O_2$ was considered as the main ROS [139]. Wang et al. and Yang et al. prepared sludge-derived biochar and Co-impregnated biochar to active PMS, and the •OH and $SO_4^{\bullet -}$ were considered as the dominant ROS, respectively [88, 140]. However, the reasons for the dominant role of each ROS and the dynamic relationship with the species of biochar-based catalysts still need to be constructed in the future.

In the activation process of PMS, biochar-based catalysts can be used as both electron acceptors and electron donors. The production of ROS is closely related to the role played by biochar-based catalysts. Fig. 5 showed the generation pathway of

ROS. Biochar-based catalysts are used as electron donors in the production of $SO_4^{\bullet -}$ and • OH. The electron donation of biochar-based catalysts is closely related to PFRs, structural defects and oxygen-containing functional groups. Jiang et al. reported that the $SO_4^{\bullet -}$ and •OH can be generated by the reaction between PFRs and PMS [101]. The electrons can be transformed from PFRs in the biochar to O_2 to generate superoxide radical anions (SRA), which can be reacted with PMS, and then generated $SO_4^{\bullet -}$ [141]. Fig. 6 showed the catalytic mechanisms of pristine biochar for activating PMS and the significant role of structural defects for contaminants degradation. Biochar approaches PMS and adsorbs it on the surface of biochar firstly. The defect structures of biochar (edge defects, curvature, vacancies, etc.) can generate dangling σ bonds, which can keep the π-electrons of biochar from being limited by the edge carbon atoms, thereby transferring electrons from biochar to PMS and generate $SO_4^{\bullet -}$ and •OH [142]. Besides this, the lone pair of electrons in the Lewis basic site in the biochar-based catalysts (such as the oxygen atom in C=O, pyridinic N and pyrrolic N), and the free flowing π-electrons in the sp^2-hybridized carbon can transfer from biochar-based catalysts to PMS to induce the production of $SO_4^{\bullet -}$ and •OH. The production of $SO_4^{\bullet -}$ and •OH is shown in Eqs. (1) and (2).

When biochar-based catalysts contain variable valence metals, there will be one more way to generate radicals. M^{n+}, as an electron donor, provides an electron to the PMS and break the O-O, which results in the generation of $SO_4^{\bullet -}$. The generated $SO_4^{\bullet -}$ will further react with water to produce •OH. The produced M^{n+1} can continue to react with PMS and be reduced to M^{n+} to complete the redox cycle (Eqs. (3) - (6)).

However, it is worth noting that the reduction potential of $HSO_5^-/SO_5^{\bullet -}$ (1.1 V) is more positive than Fe^{3+}/Fe^{2+} (0.77V), the reduction of Fe^{3+} by PMS is thermodynamically unfavorable. With the exist of $O_2^{\bullet -}$ in the reaction system, the reduction potentials of $O_2^{\bullet -}/O_2$ (-0.33 V) is more negative than that of Fe^{3+}/Fe^{2+}, thus the Fe^{3+} can be reduced by the $O_2^{\bullet -}$ in the perspective of thermodynamics (Eqs. (7) - (9)).

$$HSO_5^- + e^- \rightarrow OH^- + SO_4^{\bullet -} \quad (1)$$

$$HSO_5^- + e^- \rightarrow \bullet OH + SO_4^{2-} \quad (2)$$

$$M^{n+} + HSO_5^- \rightarrow M^{n+1} + SO_4^{\bullet -} + OH^- \quad (3)$$

$$M^{n+} + HSO_5^- \rightarrow M^{n+1} + \bullet OH + SO_4^{2-} \quad (4)$$

$$M^{n+1} + HSO_5^- \rightarrow M^{n+} + SO_5^{\bullet -} + H^+ \quad (5)$$

$$SO_4^{\bullet -} + H_2O \rightarrow SO_4^{2-} + H^+ + \bullet OH \quad (6)$$

$$HSO_5^- \rightarrow H^+ + SO_5^{2-} \quad (7)$$

$$SO_5^{2-} + H_2O \rightarrow O_2^{\bullet -} + SO_4^{2-} + 2H^+ \quad (8)$$

$$Fe^{3+} + O_2^{\bullet -} \rightarrow Fe^{2+} + O_2 \quad (9)$$

It is generally believed that $^1O_2$ can be produced by PMS self-decomposition (Eqs. (7) and (10)). Besides this, biochar-based catalysts can act as electron acceptors to induce the production of $^1O_2$. Gao et al. reported that the electron-deficient C atom near graphitic N is the active site of $^1O_2$ production [143, 144]. Compared with graphitic N, the covalent radius of C atoms is larger and the electronegativity is lower [145]. Electrons can be transferred from a weakly electronegative C atom to an adjacent highly electronegative N atom. The positively-charged C atoms form an

electron-deficient environment and attract electrons from the PMS. PMS loses electrons and produce $SO_5^{\bullet -}$, the $SO_5^{\bullet -}$ would further react with H_2O to produce $^1O_2$ (Eqs. (11) and (12)). Zou et al. reported that PMS molecules can release electrons to electrophilic C=O groups to form $SO_5^{\bullet -}$, the self-reaction of $SO_5^{\bullet -}$ would produce $^1O_2$ (Eqs. (11) and (13)) [146]. Nevertheless, the mechanisms of the production of $^1O_2$ during PMS activation by biochar-based catalysts are still unclear, and more reliable active sites need to be further explored.

$$HSO_5^- + SO_5^{2-} \rightarrow SO_4^{2-} + HSO_4^- + {}^1O_2 \quad (10)$$

$$HSO_5^- \rightarrow SO_5^{\bullet -} + H^+ + e \quad (11)$$

$$2SO_5^{\bullet -} + H_2O \rightarrow 1/2\,{}^1O_2 + 2HSO_4^- \quad (12)$$

$$SO_5^{\bullet -} + SO_5^{\bullet -} \rightarrow {}^1O_2 + SO_4^- \quad (13)$$

4.2 Direct electron transfer and surface-bound reactive species

In the process of PMS activation by biochar-based catalysts, there are several special non-radical mechanisms, including surface-bound reactive species and direct electron transfer. It is worth noting that the formation of surface-bound reactive species is also classified in the non-radical mechanism. The aforementioned radicals refer to the free radicals that can exist in the bulk solution after generation. There are very few reports about surface-bound reactive species. Fu et al. confirmed the existence of surface-bound $SO_4^{\bullet -}$ and •OH through phenol quenching experiments in their experiments [147, 148]. However, the mechanism and scene of the generation of surface-bound $SO_4^{\bullet -}$ and •OH still need to be further explored.

In the direct electron transfer process, PMS is first adsorbed on the electron sites such as graphitized N on the surface of biochar. The π-π reaction between the contaminants and the carbon or oxygen functional groups of the biochar-based catalysts makes the contaminants adsorb on the biochar-based catalysts. Organic contaminants and PMS acted as electron donors and electron acceptors, respectively, and the biochar-based catalysts was the electron shuttle between organic contaminants and PMS [137, 149]. Organic contaminants lose electron to convert into intermediate products or even directly mineralized into CO_2 and H_2O. PMS gets electrons to form OH^- and SO_4^{2-} (Eqs. (14)). Direct electron transfer is a very important non-radical mechanism and can even be in a dominant position. Zhao et al. reported that when used sludge derived biochar-supported MnOx as PMS activator, direct electron transfer is the dominant PMS activation mechanism [150]. But what influences the contribution rates of various activation mechanisms? What is the dynamic relationship between the contribution rates of various activation mechanisms and biochar-based catalysts or contaminants? These problems need to be solved urgently.

$$HSO_5^- + 2e^- \rightarrow OH^- + SO_4^{2-} \qquad (14)$$

5. Effects of reaction parameters on contaminants degradation

Biochar-based catalysts can effectively activate PMS to degrade various organic contaminants such as pharmaceuticals, organic dyes, endocrine disruptors, and pesticides. Table 2 showed the performances of biochar-based catalysts as PMS activator for the degradation of various organic contaminants. Reaction conditions,

including PMS and catalysts concentration, temperature, pH, anions and NOM, all have effects on activating PMS and degrading contaminants (Fig. 7). PMS concentration and catalyst dosage have a positive effect on the degradation process, but excessive amounts will inhibit the degradation of contaminants. The increase in temperature is beneficial to the entire catalytic degradation process. The influence of pH values on the degradation of contaminants varies with the kinds of contaminants and catalysts. Most ions will inhibit the degradation of contaminants. The presence of NOM will have a dual effect on degradation. Therefore, the influence of various reaction parameters on the biochar/PMS system is worth exploring.

5.1 PMS and catalysts concentration

The presence of PMS will induce the generation of ROS, and different concentrations of PMS will have different effects on the removal rate of contaminants. Wang et al. pointed out that the degradation rate of triclosan (TCS) increased with the increase of PMS concentration but decreased when the concentration of PMS reached to 1.2 mM [88]. Fu et al. also reported that the removal rate of p-hydroxybenzoic acid (HBA) was increased first but decreased later with the increase of PMS concentration [147]. Adding PMS can provide more oxidants, thus improving the removal efficiency of contaminants, but excessive PMS can cause the self-quenching reactions of PMS. As described in Eqs. ((15)-(16)), excessive PMS will promote the conversion of •OH and $SO_4^{\bullet -}$ to $SO_5^{\bullet -}$ and HSO_4^- with lower reactivity. This is similar to the results of some previous studies [151, 152]. Therefore, choosing the optimal concentration of

PMS is crucial for practical applications [153].

$$\bullet OH + HSO_5^- \rightarrow SO_5^{\bullet -} + H_2O \quad (15)$$

$$SO_4^{\bullet -} + HSO_5^- \rightarrow SO_5^{\bullet -} + HSO_4^- \quad (16)$$

Catalysts concentration is also an important factor for the activation of PMS. Increasing the concentration of biochar-based catalysts may not only add active sites to activate PMS but also increase the react chance with contaminants molecules. In addition, increasing the concentration of biochar-based catalysts was beneficial to the generation of radical such as $SO_4^{\bullet -}$, which promoted the degradation of tetracycline (TC) [154]. However, excessive increasing biochar concentration may generate abundant oxidative radical and promoting the self-interaction between radicals (Eqs. (17-19)) [155]. Gan et al. reported that when the catalyst concentration ranged from 0.1 g/L to 0.5 g/L, the degradation rate of dimethyl phthalate (DMP) gradually increased, but it changed little when the catalyst concentration was higher than 0.5 g/L. This was due to the more reaction active sites provided by catalysts and the later quenching reactions between radicals.

$$\bullet OH + \bullet OH \rightarrow H_2O_2 \quad (17)$$

$$SO_4^{\bullet -} + SO_4^{\bullet -} \rightarrow S_2O_8^{2-} \quad (18)$$

$$SO_4^{\bullet -} + \bullet OH \rightarrow HSO_5^- \quad (19)$$

Oh et al. pointed out that during the BPA degradation process, increasing the PMS concentration less contributed to BPA degradation than increasing the catalyst dose [62]. Although increasing the concentration of PMS can enhance its reactivity and promote the degradation of contaminants, however, the limited active sites

provided by the catalyst will inevitably lead to competition between PMS molecules, which will affect the entire degradation process.

5.2 Temperature

Temperature has proven to be one of the most significant factors affecting the activation of PMS and the subsequent degradation of contaminants. Obviously, increasing reaction temperature within a certain range will improve the remove rate of contaminants. Temperature will affect the stability of PMS, and high temperature will accelerate the decomposition of PMS to ROS. Fu et al. showed that it took 6 min to completely degrade Orange II at 25 ℃, while 5 min at 45 ℃ [148]. In the Fe_3O_4-biochar/PMS reaction system, the higher the temperature, the faster of the growth rate and the larger of the size of Fe_3O_4 nanoparticles, which were conducive to the formation of the mesoporous structure of the catalyst [147]. The increase of temperature will accelerate the molecular movement and promote the mass transfer process of heterogeneous systems. Therefore, the view that the degradation rate of contaminants will increase with the increase of temperature in reasonable range has been unanimously recognized in previous studies [156, 157].

5.3 pH

The pH value of the solution is an important parameter that affects the chemical reaction [158]. It not only determines the state of the chemical substance, but also affects the surface properties of the catalysts [159]. The effects of different pH values (3-12) on the activation of PMS and subsequent degradation of contaminants by

different biochar-based catalysts have been reported by many scholars [160].

It is reported that the degradation rate of the contaminants under near-neutral conditions is higher than the conditions of overly acidic or alkaline [28]. In most cases, the degradation rate of contaminants increases when the pH increases from 2 to 8 or 9, and decreases when the pH continues to increase. That is to say, when the pH is 8 or 9, the degradation rate of contaminants is the highest [46, 58, 101, 161]. Under acidic conditions, excess H^+ will form strong hydrogen bonds with O-O in PMS, thereby inhibiting the reaction between biochar-based catalysts and PMS [162]. Ahmadiet et al. reported that high concentrations of H^+ could affect the formation of $SO_4^{\bullet -}$ and •OH [35, 163]. Under strongly alkaline conditions, more divalent PMS anions are formed [164], and electrostatic repulsive forces are generated between various negatively charged PMS components and negatively charged catalysts, preventing the generation of ROS, and further impeding the degradation of contaminants [165]. In addition, PMS will hydrolyze to form inactive materials such as SO_4^{2-} under basic conditions (Eqs. (20)). What's more, the pKa of PMS is 9.4. When the pH of the solution is higher than 9.4, PMS will have a self-decompose reaction, which will affect the activation and degradation process [166, 167].

$$HSO_5^- + 2OH^- \rightarrow 2SO_4^{2-} + H_2O + O_2 \quad (20)$$

Nevertheless, many scholars have reported that the change of pH value has no obvious effect on the degradation of contaminants [153, 168]. Hu et al. reported that this may be related to the rapid production of a large number of active species on the active sites of the biochar-supported $MnFe_2O_4$ composite catalysts [148]. Factors such

as the isoelectric point of the biochar-based catalysts and the dissociation constant of the contaminants will affect the effect of pH on PMS activation. Therefore, the effect of solution pH value on the reaction activity of the whole system varies with the kinds of contaminants and catalysts.

5.4 Anions

There are many different anions in the water environment, such as chloride (Cl^-), bicarbonate (HCO_3^-) and dihydrogen phosphate ($H_2PO_4^-$). In fact, the presence of various anions in wastewater, even at low concentrations, can potentially affect the PMS activation process [169], which may affect the generation of ROS and the degradation of contaminants [170, 171]. Since each anion has different physical and chemical properties (rate constants of radicals, existence forms, etc.), it has different influence on the elimination of contaminants.

The influence of Cl^- on the elimination of contaminants various with the type of ROS, the reaction rate between Cl^- and ROS and the activation pathways. Chen et al. reported that when the Cl^- concentration increased, the contaminant degradation rate decreased gradually [46]. Fu et al. reported that Cl^- had a significant positive effect on the remove of p-hydroxybenzoic acid [147]. Hu et al.'s research showed that the Cl^- had no significant effect on the degradation of methylene blue (MB) [172]. Cl^- was an $SO_4^{\bullet -}$ and •OH scavenger that could consume $SO_4^{\bullet -}$/•OH and produce •Cl and $HOCl^{\bullet -}$, but the reaction rate of Cl^- and $SO_4^{\bullet -}$ is 3.1×10^8 $M^{-1}s^{-1}$, which is lower than the reaction rate between Cl^- and •OH (4.3×10^9 $M^{-1}s^{-1}$) [173-176]. Besides this,

under neutral conditions, HOCl• will be converted back to •OH, while under acidic conditions, HOCl• will react with H^+ to form Cl• (Eqs. (21)-(23)). It is mentioned before that different system has different conclusions about which ROS plays a leading role, so the effect of Cl^- in different systems is not the same. In addition, the HSO_5^- can oxidize excess Cl^-, and the HOCl formed by the reaction had a strong oxidation capacity (Eqs. (24)), which could promoting the degradation of contaminants [35, 177]. When the activation mechanism is dominated by non-radical mechanism, the effect of Cl^- can be ignored naturally.

HCO_3^- and $H_2PO_4^-$ usually have a double effect on the degradation of contaminants [178]. HCO_3^- and $H_2PO_4^-$ can quench the $SO_4^{\bullet -}$ and •OH and generate $\bullet HCO_3$ and $\bullet H_2PO_4$, respectively (Eqs. (25)-(28)). But the oxidation potential of $\bullet HCO_3$ and $\bullet H_2PO_4$ is lower than that of $SO_4^{\bullet -}$ and •OH, which inhibits the reaction [30,36]. However, a large amount of HCO_3^- can adjust the pH of the system to an alkaline atmosphere at 8.5 [179], this conditions is beneficial to the conversion of HSO_5^- to SO_5^{2-} (Eqs. (27)), provide more opportunities for the generation of $^1O_2$ [180]. Furthermore, it is worth noting that the asymmetric structure of PMS makes it easy to be attacked by nucleophiles (HCO_3^-, $H_2PO_4^-$) and decompose rapidly, which means that HCO_3^- and $H_2PO_4^-$ can directly activate PMS [181]. Du et al. and Ye et al. mentioned in their researches that $H_2PO_4^-$ and HCO_3^- have a positive effect on the degradation of contaminants, respectively [82, 144]. But in most cases, $H_2PO_4^-$ and HCO_3^- still act as inhibitors.

$$SO_4^{\bullet -} + Cl^- \rightarrow SO_4^{2-} + \bullet Cl \quad (21)$$

$$\bullet OH + Cl^- \leftrightarrow HOCl^{\bullet -} \quad (22)$$

$$HOCl\bullet^- + H^+ \rightarrow \bullet Cl + H_2O \quad (23)$$

$$HSO_5^- + Cl^- \leftrightarrow SO_4^{2-} + HOCl \quad (24)$$

$$SO_4^{\bullet -} + HCO_3^- \rightarrow SO_4^{2-} + \bullet HCO_3 \text{ or}$$

$$HCO_3^- + SO_4^{\bullet -} \rightarrow SO_4^{2-} + CO_3^{\bullet -} + H^+ \quad (25)$$

$$\bullet OH + HCO_3^- \rightarrow H_2O + CO_3^{\bullet -} \quad (26)$$

$$SO_4^{\bullet -} + H_2PO_4^- \rightarrow SO_4^{2-} + \bullet H_2PO_4 \quad (27)$$

$$\bullet OH + H_2PO_4^- \rightarrow OH^- + \bullet H_2PO_4 \quad (28)$$

$$HSO_5^- + OH^- \rightarrow SO_5^{2-} + H_2O \quad (27)$$

5.5 NOM

NOM and inorganic salts are widely present in actual wastewater. The decrease of contaminants removal efficiency caused by the reaction of ROS with NOM and other background organic components has always been a challenge for the practical application of heterogeneous catalysis. On the one hand, the biochar-based catalysts can adsorb the NOM to its surface through the carboxyl and phenolic hydroxyl groups contained in the NOM, thereby blocking the active sites of the biochar-based catalysts. In addition, NOM will compete with ROS and thus acts as a radical scavenger [180]. On the other hand, phenols contained in NOM will form semiquinone radicals with hydroquinone and quinones, which can activate PMS and promote the production of $SO_4^{\bullet -}$ [182]. As is known to all, humic acid (HA), rich in carboxyl and phenolic hydroxyl groups, is a typical NOM and prevalent in aquatic environment. It has also

been reported that HA can eliminate radicals or block the normal process of contaminants degradation and the elimination rate of contaminants decreases with the increases of HA dosage [134]. This result can be attributed to HA competing with contaminants in wastewater for a limited number of ROS [148, 183]. However, the mechanism of biochar-based catalysts to activate PMS is changeable. When it comes to special non-radical mechanisms that do not contain ROS, the influence of HA is weakened [33]. Ma et al. studied human-hair-derived carbon for PMS activation to degrade BPA, however, in their studies, no inhibition was found when 5mg/L HA was added [59]. This phenomenon can be explained by the fact that the concentration of radical in the reaction system may be very low.

6. Conclusion and prospects

PMS activation by biochar-based catalysts has become a promising SR-AOPs method for organic contaminants degradation. This article summarizes the development of biochar-based materials for the activation of PMS to remove contaminants. The different activation mechanisms of pristine biochar catalysts and modified biochar-based catalysts, including radical ($SO_4^{\bullet -}$ and •OH) and non-radical ($^1O_2$ and direct electron transfer) mechanisms were described in detail. Biochar-based catalysts will be considered as a new generation of green catalysts due to their own excellent characteristics, which can avoid the leaching problem of metal-based catalysts and secondary pollution. The PMS/biochar-based catalysts system has great catalytic potential. However, there are still many key issues to be further explored.

(1) Introduce more biochar-based catalysts from various sources.

In the preparation of biochar-based catalysts, as well as PMS activators, it is important to select attractive and suitable biomass. Different biomass has its unique structure and composition, which determines the performance and function of biochar-based catalysts. According to actual application requirements, choosing the right biomass is critical. For example, when activating PMS, it is obviously desirable to select biomass that can generate biochar-based catalysts with large specific surface areas and rich active sites (such as graphite N). But this requires a systematic comparative analysis of biochar-based catalysts come from various sources, which is currently lacking. In addition, the current sources of biochar-based catalysts used to activate PMS are still limited. There are many studies on lignocellulose-rich plant-based biochar (from wood or agricultural waste), while animal-based biochar from animal manure and garbage has not been studied. The potential and research gap between animal-based biochar and plant-based biochar for PMS activation need to be researched in the further.

(2) Construct more excellent biochar-based catalysts.

The special structure (defects and graphitization) and functional groups of biochar-based catalysts that facilitate PMS activation need to be paid attention to. The types and quantities of functional groups contained in biochar-based catalysts, as well as the amount of transferrable electrons in the functional groups, will affect the catalytic performance, but there is still a lack of quantitative research in this area. The combination of heteroatoms can further enhance the catalytic activity, such as N, S, P,

B. At present, most of the studies on heteroatom doped biochar catalysts focus on the N-doped biochar, and some scholars have studied the catalytic effects of N-S co-doped biochar catalysts and N-S doped biochar-based catalysts (such as S-Co_3O_4 in N doped biochar (Co-S@NC) [82], core-shell Co@C nanoparticles with N and S into hierarchically porous biochar (Co-N-S-PCs)) [81]. In the future, doping other electron donors or receptors may be considered to improve the performance of biochar-based catalysts. Studies on biochar composite catalysts mainly focus on metal-based biochar composites with single metal species, mainly concentrate on Fe, Mn and Co. More kinds of metal (such as Cu, Ni, Zn and other metals with variable valence states) or nonmetal-based biochar composite catalysts need to be explored.

(3) Depth of surface activation mechanisms.

The surface activation mechanism of biochar-based catalysts is not fully understood. Currently, the known reaction pathways include radical pathways induced by $SO_4^{\bullet-}$ and •OH, non-radical pathways induced by $^1O_2$, and direct degradation of contaminants through surface electron shuttle. The activation mechanism that relies on the formation of PDS-biochar surface-confined complexes has not been reported in PMS/biochar-based catalysts system. The mechanism of the production of $^1O_2$ during PMS activation is still unclear, and more reliable active sites need to be further explored. Radical and non-radical pathways can coexist among various reaction systems, but often one side dominates. However, the reasons for the dominant role of each pathway and the dynamic relationship with biochar-based catalysts or contaminants types need to be further studied.

Different reaction pathways have their own unique characteristics, advantages and disadvantages. Radical pathway has higher degree of mineralization of organic contaminants but its active site is difficult to regenerate while non-radical pathway is less affected by competitive organic/inorganic components in water. However, the current research is mainly focused on identifying the reaction pathway, and the dynamic relationship between the reaction pathways and the catalysts has not been explored. At present, there are only reports of changing the pyrolysis temperature and changing the ratio of K_2FeO_4 to the pristine biochar to regulate the reaction pathway [77, 87]. It is of great significance for the application of SR-AOPs to regulate the pathway of radical and non-radical in line with the characteristics of each path and practical application requirements.

(4) The reusability of biochar-based catalysts.

In the practical applications, the reusability of biochar catalysts is one of the factors that must be considered. The deterioration of catalytic performance can be attributed to five points. Firstly, ROS will cause oxidation reaction on the surface of catalysts. Secondly, during continuous cycle operation, the catalysts will be lost, and the active sites on the catalysts surface will be consumed. Thirdly, intermediate degradation products will inhibit the active sites and block the porous structure of biochar. Fourthly, PMS or contaminants will be adsorbed on the surface of catalysts, and occur surface oxidation reaction, reducing its specific surface area. Fifthly, for N-doped biochar-based catalysts, graphitic N will be irreversibly converted to pyridine N, which will affects PMS activation efficiency. Heat treatment can remove

intermediate products that block the pore structure and active sites. But this still cannot meet actual application requirements.

(5) Application in actual water treatment.

At present, the SR-AOPs of biochar-based catalysts to activate PMS are mainly concentrated on the research level and have not been widely used in the actual engineering field. The actual problems it faces include: low catalytic activity of the pristine biochar catalysts, the influence of hetero ions and NOM in the actual wastewater, the reusability of the biochar-based catalysts, production of halogenated intermediates and sulfate ions. Developing more excellent biochar precursors and constructing modified biochar-based catalysts can solve the problem of low activity of the pristine biochar. The interference of anions and NOM is a challenge for heterogeneous catalysis. But in fact, in the non-radical pathway which does not involve radical, the interference of anions and NOM can be weakened or even ignored. The problem is that the key factors that determine the activation mechanism of PMS are still unknown. How to regulate specific activation mechanism according to actual application needs is one of the challenges facing in the future. The H_2SO_4 produced after PMS decomposition causes potential secondary contamination problems. In the standard for drinking water (GB 5749-2006), the maximum SO_4^{2-} concentration is 250 mg/L, so the dose of PMS requires to be minimized to reduce its underlying environmental hazard. As for halogenated intermediates, which has been widely concerned in SR-AOPs, it can be alleviated by adding online secondary treatment facilities or adjusting pH through kinetic control and chemical addition to inhibit the

rate of formation of halogenated intermediates.

Acknowledgements

The study was financially supported by the National Natural Science Foundation of China (51979103, 51679085, 51521006, and 51508177), the Funds of Hunan Science and Technology Innovation Project (2018RS3115, 2020RC5012).

References

[1] Y. Pan, X. Liu, W. Zhang, Z. Liu, G. Zeng, B. Shao, Q. Liang, Q. He, X. Yuan, D. Huang, M. Chen, Advances in photocatalysis based on fullerene C60 and its derivatives: Properties, mechanism, synthesis, and applications, Appl. Catal. B-Environ. 265 (2020) 118579.
[2] Y. Liu, D. Huang, M. Cheng, Z. Liu, C. Lai, C. Zhang, C. Zhou, W. Xiong, L. Qin, B. Shao, Q. Liang, Metal sulfide/MOF-based composites as visible-light-driven photocatalysts for enhanced hydrogen production from water splitting, Coord. Chem. Rev. 409 (2020) 213220.
[3] Z. Liu, Y. Liu, G. Zeng, B. Shao, M. Chen, Z. Li, Y. Jiang, Y. Liu, Y. Zhang, H. Zhong, Application of molecular docking for the degradation of organic pollutants in the environmental remediation: A review, Chemosphere 203 (2018) 139-150.
[4] Y. Liu, G. Zeng, H. Zhong, Z. Wang, Z. Liu, M. Cheng, G. Liu, X. Yang, S. Liu, Effect of rhamnolipid solubilization on hexadecane bioavailability: enhancement or reduction?, J. Hazard. Mater. 322 (2017) 394-401.
[5] B. Petrie, R. Barden, B. Kasprzyk-Hordern, A review on emerging contaminants in wastewaters and the environment: current knowledge, understudied areas and recommendations for future monitoring, Water Res. 72 (2015) 3-27.
[6] Q. Liang, X. Liu, G. Zeng, Z. Liu, L. Tang, B. Shao, Z. Zeng, W. Zhang, Y. Liu, M. Cheng, W. Tang, S. Gong, Surfactant-assisted synthesis of photocatalysts: Mechanism, synthesis, recent advances and environmental application, Chem. Eng. J. 372 (2019) 429-451.
[7] T. Wu, X. Liu, Y. Liu, M. Cheng, Z. Liu, G. Zeng, B. Shao, Q. Liang, W. Zhang, Q. He, W. Zhang, Application of QD-MOF composites for photocatalysis: Energy production and environmental remediation, Coord. Chem. Rev. 403 (2020) 213097.
[8] B. Shao, J. Wang, Z. Liu, G. Zeng, L. Tang, Q. Liang, Q. He, T. Wu, Y. Liu, X. Yuan, $Ti_3C_2T_x$ MXene decorated black phosphorus nanosheets with improved visible-light photocatalytic activity: experimental and theoretical studies, J. Mater. Chem. A 8 (2020) 5171-5185.
[9] B. Shao, Z. Liu, G. Zeng, H. Wang, Q. Liang, Q. He, M. Cheng, C. Zhou, L. Jiang, B. Song, Two-dimensional transition metal carbide and nitride (MXene) derived quantum dots (QDs): synthesis, properties, applications and prospects, J. Mater. Chem. A 8 (2020) 7508-7535.
[10] Y.Z. Lin, L.B. Zhong, S. Dou, Z.D. Shao, Q. Liu, Y.M. Zheng, Facile synthesis of electrospun carbon nanofiber/graphene oxide composite aerogels for high efficiency oils absorption, Environ. Int. 128 (2019) 37-45.
[11] J. Huang, X. Liu, W. Zhang, Z. Liu, H. Zhong, B. Shao, Q. Liang, Y. Liu, W. Zhang, Q. He, Functionalization of covalent organic frameworks by metal modification: Construction, properties and applications, Chem. Eng. J. 404 (2021) 127136.
[12] Q. Liang, B. Shao, S. Tong, Z. Liu, L. Tang, Y. Liu, M. Cheng, Q. He, T. Wu, Y. Pan, J. Huang, Z. Peng, Recent advances of melamine self-assembled graphitic carbon nitride-based materials: Design, synthesis and application in energy and environment,

Chem. Eng. J. 405 (2021) 126951.
[13] H. Zhong, Z. Wang, Z. Liu, Y. Liu, M. Yu, G. Zeng, Degradation of hexadecane by Pseudomonas aeruginosa with the mediation of surfactants: Relation between hexadecane solubilization and bioavailability, Int. Biodeterior. Biodegradation 115 (2016) 141-145.
[14] H. Zhong, H. Zhang, Z. Liu, X. Yang, M.L. Brusseau, G. Zeng, Sub-CMC solubilization of dodecane by rhamnolipid in saturated porous media, Sci. Rep. 6 (2016) 33266.
[15] B. Shao, Z. Liu, H. Zhong, G. Zeng, G. Liu, M. Yu, Y. Liu, X. Yang, Z. Li, Z. Fang, J. Zhang, C. Zhao, Effects of rhamnolipids on microorganism characteristics and applications in composting: A review, Microbiol. Res. 200 (2017) 33-44.
[16] Z. Liu, B. Shao, G. Zeng, M. Chen, Z. Li, Y. Liu, Y. Jiang, H. Zhong, Y. Liu, M. Yan, Effects of rhamnolipids on the removal of 2,4,2,4-tetrabrominated biphenyl ether (BDE-47) by Phanerochaete chrysosporium analyzed with a combined approach of experiments and molecular docking, Chemosphere 210 (2018) 922-930.
[17] W. Zhang, Z. Zeng, Z. Liu, J. Huang, R. Xiao, B. Shao, Y. Liu, Y. Liu, W. Tang, G. Zeng, J. Gong, Q. He, Effects of carbon nanotubes on biodegradation of pollutants: Positive or negative?, Ecotoxicol. Environ. Saf. 189 (2020) 109914.
[18] H. Qingyun, P. Xu, C. Zhang, Z. Guangming, L. Zhifeng, W. Dongbo, T. Wangwang, D. Haoran, T. Xiaofei, D. Abing, Influence of surfactants on anaerobic digestion of waste activated sludge: acid and methane production and pollution removal, Crit. Rev. Biotechnol. 39 (2019).
[19] B. Shao, Z. Liu, G. Zeng, Y. Liu, X. Yang, C. Zhou, M. Chen, Y. Liu, Y. Jiang, M. Yan, Immobilization of laccase on hollow mesoporous carbon nanospheres: Noteworthy immobilization, excellent stability and efficacious for antibiotic contaminants removal, J. Hazard. Mater. 362 (2019) 318-326.
[20] Y. Liu, Z. Liu, G. Zeng, M. Chen, Y. Jiang, B. Shao, Z. Li, Y. Liu, Effect of surfactants on the interaction of phenol with laccase: Molecular docking and molecular dynamics simulation studies, J. Hazard. Mater. 357 (2018) 10-18.
[21] B. Shao, X. Liu, Z. Liu, G. Zeng, Q. Liang, C. Liang, Y. Cheng, W. Zhang, Y. Liu, S. Gong, A novel double Z-scheme photocatalyst $Ag_3PO_4/Bi_2S_3/Bi_2O_3$ with enhanced visible-light photocatalytic performance for antibiotic degradation, Chem. Eng. J. 368 (2019) 730-745.
[22] Z. Liu, Y. Jiang, X. Liu, G. Zeng, B. Shao, Y. Liu, Y. Liu, W. Zhang, W. Zhang, M. Yan, X. He, Silver chromate modified sulfur doped graphitic carbon nitride microrod composites with enhanced visible-light photoactivity towards organic pollutants degradation, Compos. Pt. B-Eng. 173 (2019) 106918.
[23] B. Shao, X. Liu, Z. Liu, G. Zeng, W. Zhang, Q. Liang, Y. Liu, Q. He, X. Yuan, D. Wang, S. Luo, S. Gong, Synthesis and characterization of 2D/0D g-C_3N_4/CdS-nitrogen doped hollow carbon spheres (NHCs) composites with enhanced visible light photodegradation activity for antibiotic, Chem. Eng. J. 374 (2019) 479-493.
[24] B. Shao, Z. Liu, G. Zeng, Z. Wu, Y. Liu, M. Cheng, M. Chen, Y. Liu, W. Zhang, H. Feng, Nitrogen-Doped Hollow Mesoporous Carbon Spheres Modified

g-C_3N_4/Bi_2O_3 Direct Dual Semiconductor Photocatalytic System with Enhanced Antibiotics Degradation under Visible Light, ACS Sustain. Chem. Eng. 6 (2018) 16424-16436.
[25] Q. Liang, X. Liu, J. Wang, Y. Liu, Z. Liu, L. Tang, B. Shao, W. Zhang, S. Gong, M. Cheng, Q. He, C. Feng, In-situ self-assembly construction of hollow tubular g-C_3N_4 isotype heterojunction for enhanced visible-light photocatalysis: Experiments and Theories, J. Hazard. Mater. (2020) 123355.
[26] Q. Zhao, Q. Mao, Y. Zhou, J. Wei, X. Liu, J. Yang, L. Luo, J. Zhang, H. Chen, H. Chen, L. Tang, Metal-free carbon materials-catalyzed sulfate radical-based advanced oxidation processes: A review on heterogeneous catalysts and applications, Chemosphere 189 (2017) 224-238.
[27] J.L. Wang, L.J. Xu, Advanced Oxidation Processes for Wastewater Treatment: Formation of Hydroxyl Radical and Application, Critical Reviews in Environmental Science and Technology 42 (2012) 251-325.
[28] P. Hu, M. Long, Cobalt-catalyzed sulfate radical-based advanced oxidation: A review on heterogeneous catalysts and applications, Appl. Catal. B-Environ. 181 (2016) 103-117.
[29] J. Wang, S. Wang, Activation of persulfate (PS) and peroxymonosulfate (PMS) and application for the degradation of emerging contaminants, Chem. Eng. J. 334 (2018) 1502-1517.
[30] Faheem, J. Du, S.H. Kim, M.A. Hassan, S. Irshad, J. Bao, Application of biochar in advanced oxidation processes: supportive, adsorptive, and catalytic role, Environ Sci Pollut Res Int 27 (2020) 37286-37312.
[31] L. Hu, P. Wang, T. Shen, Q. Wang, X. Wang, P. Xu, Q. Zheng, G. Zhang, The application of microwaves in sulfate radical-based advanced oxidation processes for environmental remediation: A review, Sci Total Environ 722 (2020) 137831.
[32] S. Guerra-Rodríguez, E. Rodríguez, D.N. Singh, J. Rodríguez-Chueca, Assessment of Sulfate Radical-Based Advanced Oxidation Processes for Water and Wastewater Treatment: A Review, Water 10 (2018) 1828.
[33] J. Lee, U. von Gunten, J.H. Kim, Persulfate-Based Advanced Oxidation: Critical Assessment of Opportunities and Roadblocks, Environ Sci Technol 54 (2020) 3064-3081.
[34] X. Duan, H. Sun, S. Wang, Metal-Free Carbocatalysis in Advanced Oxidation Reactions, Acc. Chem. Res. 51 (2018) 678-687.
[35] F. Ghanbari, M. Moradi, Application of peroxymonosulfate and its activation methods for degradation of environmental organic pollutants: Review, Chem. Eng. J. 310 (2017) 41-62.
[36] S. Xiao, M. Cheng, H. Zhong, Z. Liu, Y. Liu, X. Yang, Q. Liang, Iron-mediated activation of persulfate and peroxymonosulfate in both homogeneous and heterogeneous ways: A review, Chem. Eng. J. (2019) 123265.
[37] E.-T. Yun, G.-H. Moon, H. Lee, T.H. Jeon, C. Lee, W. Choi, J. Lee, Oxidation of organic pollutants by peroxymonosulfate activated with low-temperature-modified nanodiamonds: Understanding the reaction kinetics and mechanism, Appl. Catal. B-Environ. 237 (2018) 432-441.

[38] T.D. Minh, M.C. Ncibi, V. Srivastava, S.K. Thangaraj, J. Jänis, M. Sillanpää, Gingerbread ingredient-derived carbons-assembled CNT foam for the efficient peroxymonosulfate-mediated degradation of emerging pharmaceutical contaminants, Appl. Catal. B-Environ. 244 (2019) 367-384.
[39] Y. Gao, Y. Zhu, L. Lyu, Q. Zeng, X. Xing, C. Hu, Electronic Structure Modulation of Graphitic Carbon Nitride by Oxygen Doping for Enhanced Catalytic Degradation of Organic Pollutants through Peroxymonosulfate Activation, Environ. Sci. Technol. 52 (2018) 14371-14380.
[40] Y. Shang, C. Chen, P. Zhang, Q. Yue, Y. Li, B. Gao, X. Xu, Removal of sulfamethoxazole from water via activation of persulfate by Fe_3C@NCNTs including mechanism of radical and nonradical process, Chem. Eng. J. 375 (2019) 122004.
[41] P.J. Duan, T.F. Ma, Y. Yue, Y.W. Li, X. Zhang, Y.A. Shang, B.Y. Gao, Q.Z. Zhang, Q.Y. Yue, X. Xu, Fe/Mn nanoparticles encapsulated in nitrogen-doped carbon nanotubes as a peroxymonosulfate activator for acetamiprid degradation, Environmental Science-Nano 6 (2019) 1799-1811.
[42] Z. Peng, X. Liu, W. Zhang, Z. Zeng, Z. Liu, C. Zhang, Y. Liu, B. Shao, Q. Liang, W. Tang, X. Yuan, Advances in the application, toxicity and degradation of carbon nanomaterials in environment: A review, Environ. Int. 134 (2020) 105298.
[43] J.M. Dangwang Dikdim, Y. Gong, G.B. Noumi, J.M. Sieliechi, X. Zhao, N. Ma, M. Yang, J.B. Tchatchueng, Peroxymonosulfate improved photocatalytic degradation of atrazine by activated carbon/graphitic carbon nitride composite under visible light irradiation, Chemosphere 217 (2019) 833-842.
[44] S. Wang, L. Xu, J. Wang, Nitrogen-doped graphene as peroxymonosulfate activator and electron transfer mediator for the enhanced degradation of sulfamethoxazole, Chem. Eng. J. 375 (2019) 122041.
[45] X. Chen, W.-D. Oh, T.-T. Lim, Graphene- and CNTs-based carbocatalysts in persulfates activation: Material design and catalytic mechanisms, Chem. Eng. J. 354 (2018) 941-976.
[46] L. Chen, S. Yang, X. Zuo, Y. Huang, T. Cai, D. Ding, Biochar modification significantly promotes the activity of Co_3O_4 towards heterogeneous activation of peroxymonosulfate, Chem. Eng. J. 354 (2018) 856-865.
[47] K. Zhu, X. Wang, D. Chen, W. Ren, H. Lin, H. Zhang, Wood-based biochar as an excellent activator of peroxydisulfate for Acid Orange 7 decolorization, Chemosphere 231 (2019) 32-40.
[48] G. Ma, Q. Yang, K. Sun, H. Peng, F. Ran, X. Zhao, Z. Lei, Nitrogen-doped porous carbon derived from biomass waste for high-performance supercapacitor, Bioresour. Technol. 197 (2015) 137-142.
[49] T. Chen, Z. Zhou, R. Han, R. Meng, H. Wang, W. Lu, Adsorption of cadmium by biochar derived from municipal sewage sludge: Impact factors and adsorption mechanism, Chemosphere 134 (2015) 286-293.
[50] S. Yang, L. Li, T. Xiao, Y. Zhang, D. Zheng, Promoting effect of ammonia modification on activated carbon catalyzed peroxymonosulfate oxidation, Sep. Purif. Technol. 160 (2016) 81-88.
[51] J. Wang, S. Wang, Preparation, modification and environmental application of

biochar: A review, J. Clean. Prod. 227 (2019) 1002-1022.
[52] L. Peng, Y. Shang, B. Gao, X. Xu, Co_3O_4 anchored in N, S heteroatom co-doped porous carbons for degradation of organic contaminant: role of pyridinic N-Co binding and high tolerance of chloride, Appl. Catal. B-Environ. 282 (2021) 119484.
[53] C. Chen, T. Ma, Y. Shang, B. Gao, B. Jin, H. Dan, Q. Li, Q. Yue, Y. Li, Y. Wang, X. Xu, In-situ pyrolysis of Enteromorpha as carbocatalyst for catalytic removal of organic contaminants: Considering the intrinsic N/Fe in Enteromorpha and non-radical reaction, Appl. Catal. B-Environ. 250 (2019) 382-395.
[54] X.-H. Dai, H.-X. Fan, C.-Y. Yi, B. Dong, S.-J. Yuan, Solvent-free synthesis of a 2D biochar stabilized nanoscale zerovalent iron composite for the oxidative degradation of organic pollutants, J. Mater. Chem. A 7 (2019) 6849-6858.
[55] D. Ding, S. Yang, X. Qian, L. Chen, T. Cai, Nitrogen-doping positively whilst sulfur-doping negatively affect the catalytic activity of biochar for the degradation of organic contaminant, Appl. Catal. B-Environ. (2019) 118348.
[56] C.D. Dong, C.W. Chen, C.M. Hung, Synthesis of magnetic biochar from bamboo biomass to activate persulfate for the removal of polycyclic aromatic hydrocarbons in marine sediments, Bioresour. Technol. 245 (2017) 188-195.
[57] H. Zhang, L. Tang, J. Wang, J. Yu, H. Feng, Y. Lu, Y. Chen, Y. Liu, J. Wang, Q. Xie, Enhanced surface activation process of persulfate by modified bagasse biochar for degradation of phenol in water and soil: Active sites and electron transfer mechanism, Colloids and Surfaces A: Physicochemical and Engineering Aspects 599 (2020) 124904.
[58] C. Liu, L. Chen, D. Ding, T. Cai, From rice straw to magnetically recoverable nitrogen doped biochar: Efficient activation of peroxymonosulfate for the degradation of metolachlor, Appl. Catal. B-Environ. 254 (2019) 312-320.
[59] W. Ma, N. Wang, Y. Du, P. Xu, B. Sun, L. Zhang, K.-Y.A. Lin, Human-Hair-Derived N, S-Doped Porous Carbon: An Enrichment and Degradation System for Wastewater Remediation in the Presence of Peroxymonosulfate, ACS Sustain. Chem. Eng. 7 (2018) 2718-2727.
[60] S. Huang, T. Wang, K. Chen, M. Mei, J. Liu, J. Li, Engineered biochar derived from food waste digestate for activation of peroxymonosulfate to remove organic pollutants, Waste Manag 107 (2020) 211-218.
[61] Z. Li, K. Li, S. Ma, B. Dang, Y. Li, H. Fu, J. Du, Q. Meng, Activation of peroxymonosulfate by iron-biochar composites: Comparison of nanoscale Fe with single-atom Fe, J Colloid Interface Sci 582 (2021) 598-609.
[62] W.-D. Oh, A. Veksha, X. Chen, R. Adnan, J.-W. Lim, K.-H. Leong, T.-T. Lim, Catalytically active nitrogen-doped porous carbon derived from biowastes for organics removal via peroxymonosulfate activation, Chem. Eng. J. 374 (2019) 947-957.
[63] A. Brandt, L. Chen, B.E. van Dongen, T. Welton, J.P. Hallett, Structural changes in lignins isolated using an acidic ionic liquid water mixture, Green Chem. 17 (2015) 5019-5034.
[64] H. Meng, C. Nie, W. Li, X. Duan, B. Lai, Z. Ao, S. Wang, T. An, Insight into the effect of lignocellulosic biomass source on the performance of biochar as persulfate

activator for aqueous organic pollutants remediation: Epicarp and mesocarp of citrus peels as examples, J Hazard Mater 399 (2020) 123043.
[65] P.V. Nidheesh, A. Gopinath, N. Ranjith, A. Praveen Akre, V. Sreedharan, M. Suresh Kumar, Potential role of biochar in advanced oxidation processes: A sustainable approach, Chem. Eng. J. 405 (2021) 126582.
[66] F. Yang, S. Zhang, Y. Sun, D.C.W. Tsang, K. Cheng, Y.S. Ok, Assembling biochar with various layered double hydroxides for enhancement of phosphorus recovery, J. Hazard. Mater. 365 (2019) 665-673.
[67] S. Meyer, B. Glaser, P. Quicker, Technical, economical, and climate-related aspects of biochar production technologies: a literature review, Environ Sci Technol 45 (2011) 9473-9483.
[68] A. Tomczyk, Z. Sokołowska, P. Boguta, Biochar physicochemical properties: pyrolysis temperature and feedstock kind effects, Reviews in Environmental Science and Bio/Technology 19 (2020) 191-215.
[69] R.-y. Shi, Z.-n. Hong, J.-y. Li, J. Jiang, M.A. Kamran, R.-k. Xu, W. Qian, Peanut straw biochar increases the resistance of two Ultisols derived from different parent materials to acidification: A mechanism study, J. Environ. Manage. 210 (2018) 171-179.
[70] V. Hansen, D. Müller-Stöver, L.J. Munkholm, C. Peltre, H. Hauggaard-Nielsen, L.S. Jensen, The effect of straw and wood gasification biochar on carbon sequestration, selected soil fertility indicators and functional groups in soil: An incubation study, Geoderma 269 (2016) 99-107.
[71] K. Wiedner, C. Rumpel, C. Steiner, A. Pozzi, R. Maas, B. Glaser, Chemical evaluation of chars produced by thermochemical conversion (gasification, pyrolysis and hydrothermal carbonization) of agro-industrial biomass on a commercial scale, Biomass Bioenerg. 59 (2013) 264-278.
[72] G. Gasco, J. Paz-Ferreiro, M.L. Alvarez, A. Saa, A. Mendez, Biochars and hydrochars prepared by pyrolysis and hydrothermal carbonisation of pig manure, Waste Manag. 79 (2018) 395-403.
[73] P. Regmi, J.L. Garcia Moscoso, S. Kumar, X. Cao, J. Mao, G. Schafran, Removal of copper and cadmium from aqueous solution using switchgrass biochar produced via hydrothermal carbonization process, J. Environ. Manage. 109 (2012) 61-69.
[74] P. Gao, D. Yao, Y. Qian, S. Zhong, L. Zhang, G. Xue, H. Jia, Factors controlling the formation of persistent free radicals in hydrochar during hydrothermal conversion of rice straw, Environ. Chem. Lett. 16 (2018) 1463-1468.
[75] H. Lyu, B. Gao, F. He, A.R. Zimmerman, C. Ding, J. Tang, J.C. Crittenden, Experimental and modeling investigations of ball-milled biochar for the removal of aqueous methylene blue, Chem. Eng. J. 335 (2018) 110-119.
[76] J.S. Cha, S.H. Park, S.-C. Jung, C. Ryu, J.-K. Jeon, M.-C. Shin, Y.-K. Park, Production and utilization of biochar: A review, J. Ind. Eng. Chem. 40 (2016) 1-15.
[77] K. Li, S. Ma, S. Xu, H. Fu, Z. Li, Y. Li, S. Liu, J. Du, The mechanism changes during bisphenol A degradation in three iron functionalized biochar/peroxymonosulfate systems: The crucial roles of iron contents and graphitized carbon layers, J. Hazard. Mater. 404 (2020) 124145.

[78] J. Raudlatul Jannah Zaenia, J.-W. Lim, Z. Wang, D. Ding, Y.-S. Chua, S.-L. Ng, W.-D. Oh, In situ nitrogen functionalization of biochar via one-pot synthesis for catalytic peroxymonosulfate activation: Characteristics and performance studies, Sep. Purif. Technol. 241 (2020) 116702.
[79] L. Xu, C. Wu, P. Liu, X. Bai, X. Du, P. Jin, L. Yang, X. Jin, X. Shi, Y. Wang, Peroxymonosulfate activation by nitrogen-doped biochar from sawdust for the efficient degradation of organic pollutants, Chem. Eng. J. 387 (2020) 124065.
[80] H. Wang, W. Guo, B. Liu, Q. Si, H. Luo, Q. Zhao, N. Ren, Sludge-derived biochar as efficient persulfate activators: Sulfurization-induced electronic structure modulation and disparate nonradical mechanisms, Appl. Catal. B-Environ. 279 (2020) 119361.
[81] W. Tian, H. Zhang, Z. Qian, T. Ouyang, H. Sun, J. Qin, M.O. Tadé, S. Wang, Bread-making synthesis of hierarchically Co@C nanoarchitecture in heteroatom doped porous carbons for oxidative degradation of emerging contaminants, Appl. Catal. B-Environ. 225 (2018) 76-83.
[82] W. Du, Q. Zhang, Y. Shang, W. Wang, Q. Li, Q. Yue, B. Gao, X. Xu, Sulfate saturated biosorbent-derived Co-S@NC nanoarchitecture as an efficient catalyst for peroxymonosulfate activation, Appl. Catal. B-Environ. 262 (2020) 118302.
[83] Y. Li, S. Ma, S. Xu, H. Fu, Z. Li, K. Li, K. Sheng, J. Du, X. Lu, X. Li, S. Liu, Novel magnetic biochar as an activator for peroxymonosulfate to degrade bisphenol A: Emphasizing the synergistic effect between graphitized structure and $CoFe_2O_4$, Chem. Eng. J. 387 (2020) 124094.
[84] F.R. Amin, Y. Huang, Y. He, R. Zhang, G. Liu, C. Chen, Biochar applications and modern techniques for characterization, Clean Technol. Environ. Policy 18 (2016) 1457-1473.
[85] B.P. Singh, A.L. Cowie, R.J. Smernik, Biochar carbon stability in a clayey soil as a function of feedstock and pyrolysis temperature, Environ. Sci. Technol. 46 (2012) 11770-11778.
[86] D. Ouyang, Y. Chen, J. Yan, L. Qian, L. Han, M. Chen, Activation mechanism of peroxymonosulfate by biochar for catalytic degradation of 1,4-dioxane: Important role of biochar defect structures, Chem. Eng. J. 370 (2019) 614-624.
[87] J. Yu, L. Tang, Y. Pang, G. Zeng, H. Feng, J. Zou, J. Wang, C. Feng, X. Zhu, X. Ouyang, J. Tan, Hierarchical porous biochar from shrimp shell for persulfate activation: A two-electron transfer path and key impact factors, Appl. Catal. B-Environ. 260 (2020) 118160.
[88] S. Wang, J. Wang, Activation of peroxymonosulfate by sludge-derived biochar for the degradation of triclosan in water and wastewater, Chem. Eng. J. 356 (2019) 350-358.
[89] G. Wang, S. Chen, X. Quan, H. Yu, Y. Zhang, Enhanced activation of peroxymonosulfate by nitrogen doped porous carbon for effective removal of organic pollutants, Carbon 115 (2017) 730-739.
[90] L. Leng, H. Huang, An overview of the effect of pyrolysis process parameters on biochar stability, Bioresour. Technol. 270 (2018) 627-642.
[91] J. Kim, K.-H. Kim, E.E. Kwon, Enhanced thermal cracking of VOCs evolved

from the thermal degradation of lignin using CO_2, Energy 100 (2016) 51-57.
[92] E.E. Kwon, S.H. Cho, S. Kim, Synergetic sustainability enhancement via utilization of carbon dioxide as carbon neutral chemical feedstock in the thermo-chemical processing of biomass, Environ. Sci. Technol. 49 (2015) 5028-5034.
[93] E.E. Kwon, E.C. Jeon, M.J. Castaldi, Y.J. Jeon, Effect of carbon dioxide on the thermal degradation of lignocellulosic biomass, Environ. Sci. Technol. 47 (2013) 10541-10547.
[94] Butterman, H. C, M.J. Castaldi., CO_2 as a carbon neutral fuel source via enhanced biomass gasification, Environ. Sci. Technol. 43 (2009) 9030-9037.
[95] J. Wang, Z. Liao, J. Ifthikar, L. Shi, Y. Du, J. Zhu, S. Xi, Z. Chen, Z. Chen, Treatment of refractory contaminants by sludge-derived biochar/persulfate system via both adsorption and advanced oxidation process, Chemosphere 185 (2017) 754-763.
[96] H. Zhang, G. Xue, H. Chen, X. Li, Magnetic biochar catalyst derived from biological sludge and ferric sludge using hydrothermal carbonization: Preparation, characterization and its circulation in Fenton process for dyeing wastewater treatment, Chemosphere 191 (2018) 64-71.
[97] P.T. Huong, K. Jitae, T.M. Al Tahtamouni, N. Le Minh Tri, H.-H. Kim, K.H. Cho, C. Lee, Novel activation of peroxymonosulfate by biochar derived from rice husk toward oxidation of organic contaminants in wastewater, J. Water Process. Eng. 33 (2020) 101037.
[98] G. Fang, J. Gao, C. Liu, D.D. Dionysiou, Y. Wang, D. Zhou, Key role of persistent free radicals in hydrogen peroxide activation by biochar: implications to organic contaminant degradation, Environ. Sci. Technol. 48 (2014) 1902-1910.
[99] G. Fang, C. Liu, J. Gao, D.D. Dionysiou, D. Zhou, Manipulation of persistent free radicals in biochar to activate persulfate for contaminant degradation, Environ. Sci. Technol. 49 (2015) 5645-5653.
[100] L. Khachatryan, B. Dellinger, Environmentally Persistent Free Radicals (EPFRs)-2. Are Free Hydroxyl Radicals Generated in Aqueous Solutions?, Environ. Sci. Technol. 45 (2011) 9232-9239.
[101] S.-F. Jiang, L.-L. Ling, W.-J. Chen, W.-J. Liu, D.-C. Li, H. Jiang, High efficient removal of bisphenol A in a peroxymonosulfate/iron functionalized biochar system: Mechanistic elucidation and quantification of the contributors, Chem. Eng. J. 359 (2019) 572-583.
[102] L. Klupfel, M. Keiluweit, M. Kleber, M. Sander, Redox properties of plant biomass-derived black carbon (biochar), Environ. Sci. Technol. 48 (2014) 5601-5611.
[103] A. Kappler, M.L. Wuestner, A. Ruecker, J. Harter, M. Halama, S. Behrens, Biochar as an Electron Shuttle between Bacteria and Fe(III) Minerals, Environ. Sci. Technol. Lett. 1 (2014) 339-344.
[104] S. Banerjee, T. Hemraj-Benny, S.S. Wong, Covalent Surface Chemistry of Single-Walled Carbon Nanotubes, Adv. Mater. 17 (2005) 17-29.
[105] Y.N. Liang, W.-D. Oh, Y. Li, X. Hu, Nanocarbons as platforms for developing novel catalytic composites: overview and prospects, Appl. Catal. A-Gen. 562 (2018) 94-105.
[106] C. Liu, Y. Wang, Y. Zhang, R. Li, W. Meng, Z. Song, F. Qi, B. Xu, W. Chu, D.

Yuan, B. Yu, Enhancement of Fe@porous carbon to be an efficient mediator for peroxymonosulfate activation for oxidation of organic contaminants: Incorporation NH2-group into structure of its MOF precursor, Chem. Eng. J. 354 (2018) 835-848.
[107] R.-Z. Wang, D.-L. Huang, Y.-G. Liu, C. Zhang, C. Lai, X. Wang, G.-M. Zeng, X.-M. Gong, A. Duan, Q. Zhang, P. Xu, Recent advances in biochar-based catalysts: Properties, applications and mechanisms for pollution remediation, Chem. Eng. J. 371 (2019) 380-403.
[108] L. Gan, Q. Zhong, A. Geng, L. Wang, C. Song, S. Han, J. Cui, L. Xu, Cellulose derived carbon nanofiber: A promising biochar support to enhance the catalytic performance of $CoFe_2O_4$ in activating peroxymonosulfate for recycled dimethyl phthalate degradation, Sci. Total Environ. 694 (2019) 133705.
[109] X. Tan, Y. Liu, G. Zeng, X. Wang, X. Hu, Y. Gu, Z. Yang, Application of biochar for the removal of pollutants from aqueous solutions, Chemosphere 125 (2015) 70-85.
[110] M.S. Akplea, J. Lowa, S. Liua, B. Cheng, J. Yua, W. Hob, Fabrication and enhanced CO_2 reduction performance of N-self-doped TiO_2 microsheet photocatalyst by bi-cocatalyst modification, J. CO2 Util. 16 (2016) 442-449.
[111] X. Li, Y. Fang, S. Zhao, J. Wu, F. Li, M. Tian, X. Long, J. Jin, J. Ma, Nitrogen-doped mesoporous carbon nanosheet/carbon nanotube hybrids as metal-free bi-functional electrocatalysts for water oxidation and oxygen reduction, J. Mater. Chem. A 4 (2016) 13133-13141.
[112] S. Liu, J. Xia, J. Yu, Amine-Functionalized Titanate Nanosheet-Assembled Yolk@Shell Microspheres for Efficient Cocatalyst-Free Visible-Light Photocatalytic CO_2 Reduction, ACS Appl. Mater. Interfaces 7 (2015) 8166-8175.
[113] W. Xia, R. Zou, L. An, D. Xia, S. Guo, A metal–organic framework route to in situ encapsulation of $Co@Co_3O_4@C$ core@bishell nanoparticles into a highly ordered porous carbon matrix for oxygen reduction, Energy Environ. Sci. 8 (2015) 568-576.
[114] D. Deng, L. Yu, X. Chen, G. Wang, L. Jin, X. Pan, J. Deng, G. Sun, X. Bao, Iron encapsulated within pod-like carbon nanotubes for oxygen reduction reaction, Angew. Chem. Int. Ed. 52 (2013) 371-375.
[115] X. Duan, S. Indrawirawan, H. Sun, S. Wang, Effects of nitrogen-, boron-, and phosphorus-doping or codoping on metal-free graphene catalysis, Catal. Today 249 (2015) 184-191.
[116] P. Liang, C. Zhang, X. Duan, H. Sun, S. Liu, M.O. Tade, S. Wang, N-Doped Graphene from Metal–Organic Frameworks for Catalytic Oxidation of p-Hydroxylbenzoic Acid: N-Functionality and Mechanism, ACS Sustain. Chem. Eng. 5 (2017) 2693-2701.
[117] X. Wang, Y. Qin, L. Zhu, H. Tang, Nitrogen-Doped Reduced Graphene Oxide as a Bifunctional Material for Removing Bisphenols: Synergistic Effect between Adsorption and Catalysis, Environ. Sci. Technol. 49 (2015) 6855-6864.
[118] S. Inamdar, H.-S. Choi, P. Wang, M.Y. Song, J.-S. Yu, Sulfur-containing carbon by flame synthesis as efficient metal-free electrocatalyst for oxygen reduction reaction, Electrochem. Commun. 30 (2013) 9-12.
[119] H. Sun, Y. Wang, S. Liu, L. Ge, L. Wang, Z. Zhu, S. Wang, Facile synthesis of

nitrogen doped reduced graphene oxide as a superior metal-free catalyst for oxidation, Chem. Commun. 49 (2013) 9914-9916.
[120] Y. Cao, H. Yu, J. Tan, F. Peng, H. Wang, J. Li, W. Zheng, N.-B. Wong, Nitrogen-, phosphorous- and boron-doped carbon nanotubes as catalysts for the aerobic oxidation of cyclohexane, Carbon 57 (2013) 433-442.
[121] X. Duan, Z. Ao, H. Sun, S. Indrawirawan, Y. Wang, J. Kang, F. Liang, Z.H. Zhu, S. Wang, Nitrogen-doped graphene for generation and evolution of reactive radicals by metal-free catalysis, ACS Appl. Mater. Interfaces 7 (2015) 4169-4178.
[122] S. Indrawirawan, H. Sun, X. Duan, S. Wang, Low temperature combustion synthesis of nitrogen-doped graphene for metal-free catalytic oxidation, J. Mater. Chem. A 3 (2015) 3432-3440.
[123] X. Duan, Z. Ao, D. Li, H. Sun, L. Zhou, A. Suvorova, M. Saunders, G. Wang, S. Wang, Surface-tailored nanodiamonds as excellent metal-free catalysts for organic oxidation, Carbon 103 (2016) 404-411.
[124] A.C. Arampatzidou, E.A. Deliyanni, Comparison of activation media and pyrolysis temperature for activated carbons development by pyrolysis of potato peels for effective adsorption of endocrine disruptor bisphenol-A, J. Colloid Interface Sci. 466 (2016) 101-112.
[125] H. Sun, C. Kwan, A. Suvorova, H.M. Ang, M.O. Tadé, S. Wang, Catalytic oxidation of organic pollutants on pristine and surface nitrogen-modified carbon nanotubes with sulfate radicals, Appl. Catal. B-Environ. 154-155 (2014) 134-141.
[126] H. Liu, P. Sun, M. Feng, H. Liu, h. Yang, L. Wang, Z. Wang, Nitrogen and sulfur co-doped CNT-COOH as an efficient metal-free catalyst for the degradation of UV filter BP-4 based on sulfate radicals, Appl. Catal. B-Environ. 187 (2016) 1-10.
[127] H. Sun, S. Liu, G. Zhou, H.M. Ang, M.O. Tade, S. Wang, Reduced graphene oxide for catalytic oxidation of aqueous organic pollutants, ACS Appl. Mater. Interfaces 4 (2012) 5466-5471.
[128] W.-D. Oh, G. Lisak, R.D. Webster, Y.-N. Liang, A. Veksha, A. Giannis, J.G.S. Moo, J.-W. Lim, T.-T. Lim, Insights into the thermolytic transformation of lignocellulosic biomass waste to redox-active carbocatalyst: Durability of surface active sites, Appl. Catal. B-Environ. 233 (2018) 120-129.
[129] C. Wang, J. Kang, H. Sun, H.M. Ang, M.O. Tadé, S. Wang, One-pot synthesis of N-doped graphene for metal-free advanced oxidation processes, Carbon 102 (2016) 279-287.
[130] J. Liang, Y. Jiao, M. Jaroniec, S.Z. Qiao, Sulfur and Nitrogen Dual-Doped Mesoporous Graphene Electrocatalyst for Oxygen Reduction with Synergistically Enhanced Performance, Angew. Chem. Int. Ed. 51 (2012) 11496-11500.
[131] Z.-S. Wu, A. Winter, L. Chen, Y. Sun, A. Turchanin, X. Feng, K. Müllen, Three-Dimensional Nitrogen and Boron Co-doped Graphene for High-Performance All-Solid-State Supercapacitors, Adv. Mater. 24 (2012) 5130-5135.
[132] S.-A. Wohlgemuth, R.J. White, M.-G. Willinger, M.-M. Titiricia, M. Antoniettia, A one-pot hydrothermal synthesis of sulfur and nitrogen doped carbon aerogels with enhanced electrocatalytic activity in the oxygen reduction reaction, Green Chem. 14 (2012) 1515-1523.

[133] X.-f. Tan, Y.-g. Liu, Y.-l. Gu, Y. Xu, G.-m. Zeng, X.-j. Hu, S.-b. Liu, X. Wang, S.-m. Liu, J. Li, Biochar-based nano-composites for the decontamination of wastewater: A review, Bioresour. Technol. 212 (2016) 318-333.
[134] S. Wang, J. Wang, Peroxymonosulfate activation by Co_9S_8@ S and N co‐doped biochar for sulfamethoxazole degradation, Chem. Eng. J. 385 (2020) 123933.
[135] Z. Song, F. Lian, Z. Yu, L. Zhu, B. Xing, W. Qiu, Synthesis and characterization of a novel MnOx-loaded biochar and its adsorption properties for Cu^{2+} in aqueous solution, Chem. Eng. J. 242 (2014) 36-42.
[136] Y. Zhou, B. Gao, A.R. Zimmerman, H. Chen, M. Zhang, X. Cao, Biochar-supported zerovalent iron for removal of various contaminants from aqueous solutions, Bioresour. Technol. 152 (2014) 538-542.
[137] E.-T. Yun, J.H. Lee, J. Kim, H.-D. Park, J. Lee, Identifying the Nonradical Mechanism in the Peroxymonosulfate Activation Process: Singlet Oxygenation Versus Mediated Electron Transfer, Environ. Sci. Technol. 52 (2018) 7032-7042.
[138] W. Ren, G. Nie, P. Zhou, H. Zhang, X. Duan, S. Wang, The Intrinsic Nature of Persulfate Activation and N‐ Doping in Carbocatalysis, Environ. Sci. Technol. 54 (2020) 6438-6447.
[139] H. Sun, X. Peng, S. Zhang, S. Liu, Y. Xiong, S. Tian, J. Fang, Activation of peroxymonosulfate by nitrogen-functionalized sludge carbon for efficient degradation of organic pollutants in water, Bioresour. Technol. 241 (2017) 244-251.
[140] M.T. Yang, Y. Du, W.C. Tong, A.C.K. Yip, K.A. Lin, Cobalt-impregnated biochar produced from CO_2-mediated pyrolysis of Co/lignin as an enhanced catalyst for activating peroxymonosulfate to degrade acetaminophen, Chemosphere 226 (2019) 924-933.
[141] P. Hu, H. Su, Z. Chen, C. Yu, Q. Li, B. Zhou, P.J.J. Alvarez, M. Long, Selective Degradation of Organic Pollutants Using an Efficient Metal-Free Catalyst Derived from Carbonized Polypyrrole via Peroxymonosulfate Activation, Environ. Sci. Technol. 51 (2017) 11288-11296.
[142] X. Duan, H. Sun, J. Kang, Y. Wang, S. Indrawirawan, S. Wang, Insights into Heterogeneous Catalysis of Persulfate Activation on Dimensional-Structured Nanocarbons, ACS Catal. 5 (2015) 4629-4636.
[143] Y. Gao, Z. Chen, Y. Zhu, T. Li, C. Hu, New Insights into the Generation of Singlet Oxygen in the Metal-Free Peroxymonosulfate Activation Process: Important Role of Electron-Deficient Carbon Atoms, Environ. Sci. Technol. 54 (2020) 1232-1241.
[144] S. Ye, G. Zeng, X. Tan, H. Wu, J. Liang, B. Song, N. Tang, P. Zhang, Y. Yang, Q. Chen, X. Li, Nitrogen-doped biochar fiber with graphitization from Boehmeria nivea for promoted peroxymonosulfate activation and non-radical degradation pathways with enhancing electron transfer, Appl. Catal. B-Environ. 269 (2020) 118850.
[145] K. Gong, F. Du, Z. Xia, M. Durstock, L. Dai, Nitrogen-Doped Carbon Nanotube Arrays with High Electrocatalytic Activity for Oxygen Reduction, Science 323 (2009) 760-764.
[146] Y. Zou, W. Li, L. Yang, F. Xiao, G. An, Y. Wang, D. Wang, Activation of

peroxymonosulfate by sp^2-hybridized microalgae-derived carbon for ciprofloxacin degradation: Importance of pyrolysis temperature, Chem. Eng. J. 370 (2019) 1286-1297.
[147] H. Fu, P. Zhao, S. Xu, G. Cheng, Z. Li, Y. Li, K. Li, S. Ma, Fabrication of Fe_3O_4 and graphitized porous biochar composites for activating peroxymonosulfate to degrade p-hydroxybenzoic acid: Insights on the mechanism, Chem. Eng. J. 375 (2019) 121980.
[148] H. Fu, S. Ma, P. Zhao, S. Xu, S. Zhan, Activation of peroxymonosulfate by graphitized hierarchical porous biochar and $MnFe_2O_4$ magnetic nanoarchitecture for organic pollutants degradation: Structure dependence and mechanism, Chem. Eng. J. 360 (2019) 157-170.
[149] E.T. Yun, H.Y. Yoo, H. Bae, H.I. Kim, J. Lee, Exploring the Role of Persulfate in the Activation Process: Radical Precursor Versus Electron Acceptor, Environ. Sci. Technol. 51 (2017) 10090-10099.
[150] M.M. Mian, G. Liu, B. Fu, Y. Song, Facile synthesis of sludge-derived MnO_x-N-biochar as an efficient catalyst for peroxymonosulfate activation, Appl. Catal. B-Environ. 255 (2019) 117765.
[151] W. Ma, N. Wang, Y. Fan, T. Tong, X. Han, Y. Du, Non-radical-dominated catalytic degradation of bisphenol A by ZIF-67 derived nitrogen-doped carbon nanotubes frameworks in the presence of peroxymonosulfate, Chem. Eng. J. 336 (2018) 721-731.
[152] Y. Wang, H. Sun, H.M. Ang, M.O. Tadé, S. Wang, Magnetic Fe3O4/carbon sphere/cobalt composites for catalytic oxidation of phenol solutions with sulfate radicals, Chem. Eng. J. 245 (2014) 1-9.
[153] B.-C. Huang, J. Jiang, G.-X. Huang, H.-Q. Yu, Sludge biochar-based catalysts for improved pollutant degradation by activating peroxymonosulfate, J. Mater. Chem. A 6 (2018) 8978-8985.
[154] A. Khataee, F. Salahpour, M. Fathinia, B. Seyyedi, B. Vahid, Iron rich laterite soil with mesoporous structure for heterogeneous Fenton-like degradation of an azo dye under visible light, J. Ind. Eng. Chem. 26 (2015) 129-135.
[155] Y. Fan, W. Ma, J. He, Y. Du, CoMoO4 as a novel heterogeneous catalyst of peroxymonosulfate activation for the degradation of organic dyes, RSC Adv. 7 (2017) 36193-36200.
[156] S. Su, W. Guo, Y. Leng, C. Yi, Z. Ma, Heterogeneous activation of Oxone by $Co_{(x)}Fe_{(3-x)}O_4$ nanocatalysts for degradation of rhodamine B, J. Hazard. Mater. 244-245 (2013) 736-742.
[157] Y. Yao, Y. Cai, F. Lu, F. Wei, X. Wang, S. Wang, Magnetic recoverable $MnFe_{(2)}O_{(4)}$ and $MnFe_{(2)}O_{(4)}$-graphene hybrid as heterogeneous catalysts of peroxymonosulfate activation for efficient degradation of aqueous organic pollutants, J. Hazard. Mater. 270 (2014) 61-70.
[158] J. Wang, S. Wang, Reactive species in advanced oxidation processes: Formation, identification and reaction mechanism, Chem. Eng. J. 401 (2020) 126158.
[159] J. Deng, Y. Shao, N. Gao, C. Tan, S. Zhou, X. Hu, $CoFe_2O_4$ magnetic nanoparticles as a highly active heterogeneous catalyst of oxone for the degradation of

diclofenac in water, J. Hazard. Mater. 262 (2013) 836-844.
[160] R. Yin, W. Guo, H. Wang, J. Du, X. Zhou, Q. Wu, H. Zheng, J. Chang, N. Ren, Selective degradation of sulfonamide antibiotics by peroxymonosulfate alone: Direct oxidation and nonradical mechanisms, Chem. Eng. J. 334 (2018) 2539-2546.
[161] V.T. Nguyen, T.B. Nguyen, C.W. Chen, C.M. Hung, C.P. Huang, C.D. Dong, Cobalt-impregnated biochar (Co-SCG) for heterogeneous activation of peroxymonosulfate for removal of tetracycline in water, Bioresour. Technol. 292 (2019) 121954.
[162] Y. Du, W. Ma, P. Liu, B. Zou, J. Ma, Magnetic CoFe2O4 nanoparticles supported on titanate nanotubes ($CoFe_2O_4$/TNTs) as a novel heterogeneous catalyst for peroxymonosulfate activation and degradation of organic pollutants, J. Hazard. Mater. 308 (2016) 58-66.
[163] M. Ahmadi, F. Ghanbari, Combination of UVC-LEDs and ultrasound for peroxymonosulfate activation to degrade synthetic dye: influence of promotional and inhibitory agents and application for real wastewater, Environ. Sci. Pollut. Res. 25 (2018) 6003-6014.
[164] C. Tan, N. Gao, Y. Deng, J. Deng, S. Zhou, J. Li, X. Xin, Radical induced degradation of acetaminophen with Fe_3O_4 magnetic nanoparticles as heterogeneous activator of peroxymonosulfate, J. Hazard. Mater. 276 (2014) 452-460.
[165] Y. Ren, L. Lin, J. Ma, J. Yang, J. Feng, Z. Fan, Sulfate radicals induced from peroxymonosulfate by magnetic ferrospinel MFe_2O_4 (M = Co, Cu, Mn, and Zn) as heterogeneous catalysts in the water, Appl. Catal. B-Environ. 165 (2015) 572-578.
[166] A. Eslami, M. Hashemi, F. Ghanbari, Degradation of 4-chlorophenol using catalyzed peroxymonosulfate with nano-MnO_2/UV irradiation: Toxicity assessment and evaluation for industrial wastewater treatment, J. Clean. Prod. 195 (2018) 1389-1397.
[167] A. Rastogi, S.R. Al-Abed, D.D. Dionysiou, Sulfate radical-based ferrous–peroxymonosulfate oxidative system for PCBs degradation in aqueous and sediment systems, Appl. Catal. B-Environ. 85 (2009) 171-179.
[168] W. Hu, Y. Xie, S. Lu, P. Li, T. Xie, Y. Zhang, Y. Wang, One-step synthesis of nitrogen-doped sludge carbon as a bifunctional material for the adsorption and catalytic oxidation of organic pollutants, Sci. Total Environ. 680 (2019) 51-60.
[169] Y. Guo, Z. Zeng, Y. Liu, Z. Huang, Y. Cui, J. Yang, One-pot synthesis of sulfur doped activated carbon as a superior metal-free catalyst for the adsorption and catalytic oxidation of aqueous organics, J. Mater. Chem. A 6 (2018) 4055-4067.
[170] L. Hu, G. Zhang, M. Liu, Q. Wang, P. Wang, Enhanced degradation of Bisphenol A (BPA) by peroxymonosulfate with Co_3O_4-Bi_2O_3 catalyst activation: Effects of pH, inorganic anions, and water matrix, Chem. Eng. J. 338 (2018) 300-310.
[171] J. Zhou, J. Xiao, D. Xiao, Y. Guo, C. Fang, X. Lou, Z. Wang, J. Liu, Transformations of chloro and nitro groups during the peroxymonosulfate-based oxidation of 4-chloro-2-nitrophenol, Chemosphere 134 (2015) 446-451.
[172] S. Padmaja, P. Neta, R.E. Huie, Rate constants for some reactions of inorganic radicals with inorganic ions. Temperature and solvent dependence, Int. J. Chem. Kinet. 25 (1993).

[173] R. Yuan, S.N. Ramjaun, Z. Wang, J. Liu, Effects of chloride ion on degradation of Acid Orange 7 by sulfate radical-based advanced oxidation process: implications for formation of chlorinated aromatic compounds, J. Hazard. Mater. 196 (2011) 173-179.
[174] Y.H. Huang, Y.F. Huang, C.I. Huang, C.Y. Chen, Efficient decolorization of azo dye Reactive Black B involving aromatic fragment degradation in buffered Co^{2+}/PMS oxidative processes with a ppb level dosage of Co^{2+}-catalyst, J. Hazard. Mater. 170 (2009) 1110-1118.
[175] Z. Wang, R. Yuan, Y. Guo, L. Xu, J. Liu, Effects of chloride ions on bleaching of azo dyes by Co^{2+}/oxone reagent: kinetic analysis, J. Hazard. Mater. 190 (2011) 1083-1087.
[176] J. Ma, Y. Yang, X. Jiang, Z. Xie, X. Li, C. Chen, H. Chen, Impacts of inorganic anions and natural organic matter on thermally activated persulfate oxidation of BTEX in water, Chemosphere 190 (2018) 296-306.
[177] F.J. Rivas, R.R. Solís, Chloride promoted oxidation of tritosulfuron by peroxymonosulfate, Chem. Eng. J. 349 (2018) 728-736.
[178] S. Zhu, X. Huang, F. Ma, L. Wang, X. Duan, S. Wang, Catalytic Removal of Aqueous Contaminants on N-Doped Graphitic Biochars: Inherent Roles of Adsorption and Nonradical Mechanisms, Environ. Sci. Technol. 52 (2018) 8649-8658.
[179] X. Duan, Z. Ao, L. Zhou, H. Sun, G. Wang, S. Wang, Occurrence of radical and nonradical pathways from carbocatalysts for aqueous and nonaqueous catalytic oxidation, Appl. Catal. B-Environ. 188 (2016) 98-105.
[180] Y.H. Guan, J. Ma, Y.M. Ren, Y.L. Liu, J.Y. Xiao, L.Q. Lin, C. Zhang, Efficient degradation of atrazine by magnetic porous copper ferrite catalyzed peroxymonosulfate oxidation via the formation of hydroxyl and sulfate radicals, Water Res. 47 (2013) 5431-5438.
[181] M. Jiang, J. Lu, Y. Ji, D. Kong, Bicarbonate-activated persulfate oxidation of acetaminophen, Water Res 116 (2017) 324-331.
[182] B.-Z. Zhu, H.-T. Zhao, B. Kalyanaraman, B. Frei, Metal-independent production of hydroxyl radicals by halogenated quinones and hydrogen peroxide: An ESR spin trapping study, Free Radic. Biol. Med. 32 (2002) 465-473.
[183] L. Chen, D. Ding, C. Liu, H. Caia, Y. Qua, S. Yang, Y. Gao, T. Caia, Degradation of norfloxacin by $CoFe_2O_4$-GO composite coupled with peroxymonosulfat, Chem. Eng. J. 334 (2018) 273-384.
[184] M.M. Mian, G. Liu, Activation of peroxymonosulfate by chemically modified sludge biochar for the removal of organic pollutants: Understanding the role of active sites and mechanism, Chem. Eng. J. 392 (2020) 123681.
[185] Y. Xie, W. Hu, X. Wang, W. Tong, P. Li, H. Zhou, Y. Wang, Y. Zhang, Molten salt induced nitrogen-doped biochar nanosheets as highly efficient peroxymonosulfate catalyst for organic pollutant degradation, Environ. Pollut. 260 (2020) 114053.
[186] Q. Ma, L. Cui, S. Zhou, Y. Li, W. Shi, S. Ai, Iron nanoparticles in situ encapsulated in lignin-derived hydrochar as an effective catalyst for phenol removal, Environ. Sci. Pollut. Res. 25 (2018) 20833-20840.
[187] J. Yan, L. Han, W. Gao, S. Xue, M. Chen, Biochar supported nanoscale

zerovalent iron composite used as persulfate activator for removing trichloroethylene, Bioresour. Technol. 175 (2015) 269-274.
[188] Z. Li, Y. Sun, Y. Yang, Y. Han, T. Wang, J. Chen, D.C.W. Tsang, Biochar-supported nanoscale zero-valent iron as an efficient catalyst for organic degradation in groundwater, J. Hazard. Mater. 383 (2020) 121240.
[189] H. Wang, W. Guo, B. Liu, Q. Wu, H. Luo, Q. Zhao, Q. Si, F. Sseguya, N. Ren, Edge-nitrogenated biochar for efficient peroxydisulfate activation: An electron transfer mechanism, Water Res. 160 (2019) 405-414.
[190] H. Xu, Y. Zhang, J. Li, Q. Hao, X. Li, F. Liu, Heterogeneous activation of peroxymonosulfate by a biochar-supported Co_3O_4 composite for efficient degradation of chloramphenicols, Environ. Pollut. 257 (2020) 113610.
[191] L. Xu, B. Fu, Y. Sun, P. Jin, X. Bai, X. Jin, X. Shi, Y. Wang, S. Nie, Degradation of organic pollutants by Fe/N co-doped biochar via peroxymonosulfate activation: Synthesis, performance, mechanism and its potential for practical application, Chem. Eng. J. 400 (2020) 125870.
[192] Z. Huang, T. Wang, M. Shen, Z. Huang, Y. Chong, L. Cui, Coagulation treatment of swine wastewater by the method of in-situ forming layered double hydroxides and sludge recycling for preparation of biochar composite catalyst, Chem. Eng. J. 369 (2019) 784-792.
[193] R. Yin, W. Guo, H. Wang, J. Du, Q. Wu, J.-S. Chang, N. Ren, Singlet oxygen-dominated peroxydisulfate activation by sludge-derived biochar for sulfamethoxazole degradation through a nonradical oxidation pathway: Performance and mechanism, Chem. Eng. J. 357 (2019) 589-599.
[194] Z. Li, Y. Sun, Y. Yang, Y. Han, T. Wang, J. Chen, D.C.W. Tsang, Comparing biochar- and bentonite-supported Fe-based catalysts for selective degradation of antibiotics: Mechanisms and pathway, Environ. Res. 183 (2020) 109156.
[195] Z. Li, D. Liu, W. Huang, X. Wei, W. Huang, Biochar supported CuO composites used as an efficient peroxymonosulfate activator for highly saline organic wastewater treatment, Sci. Total Environ. 721 (2020) 137764.

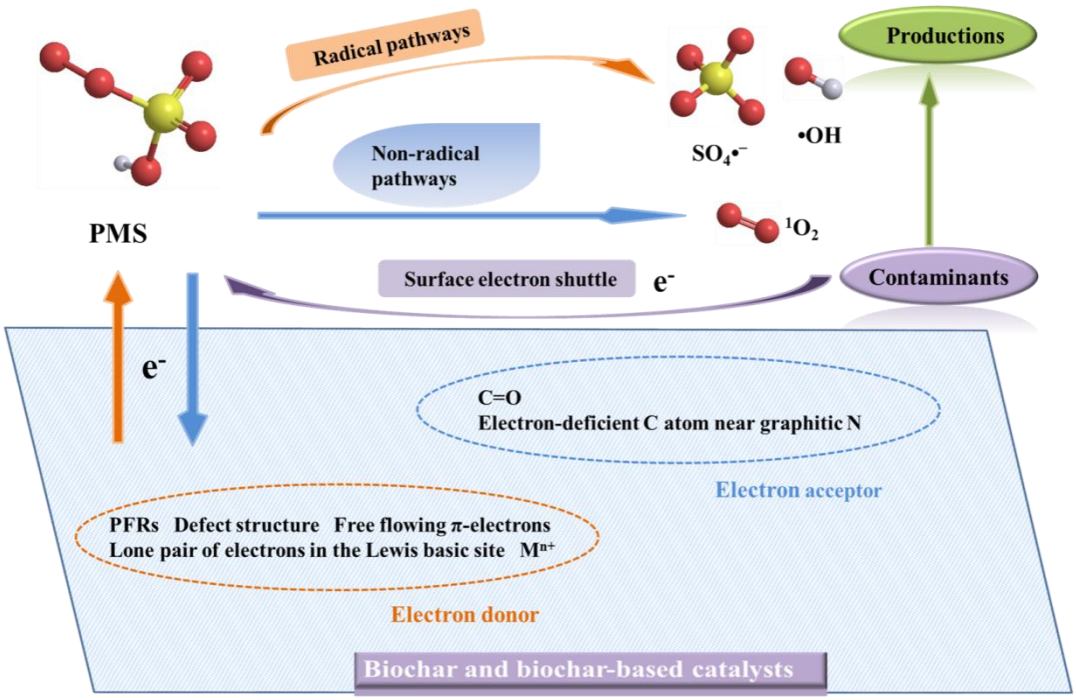

Graphical abstract

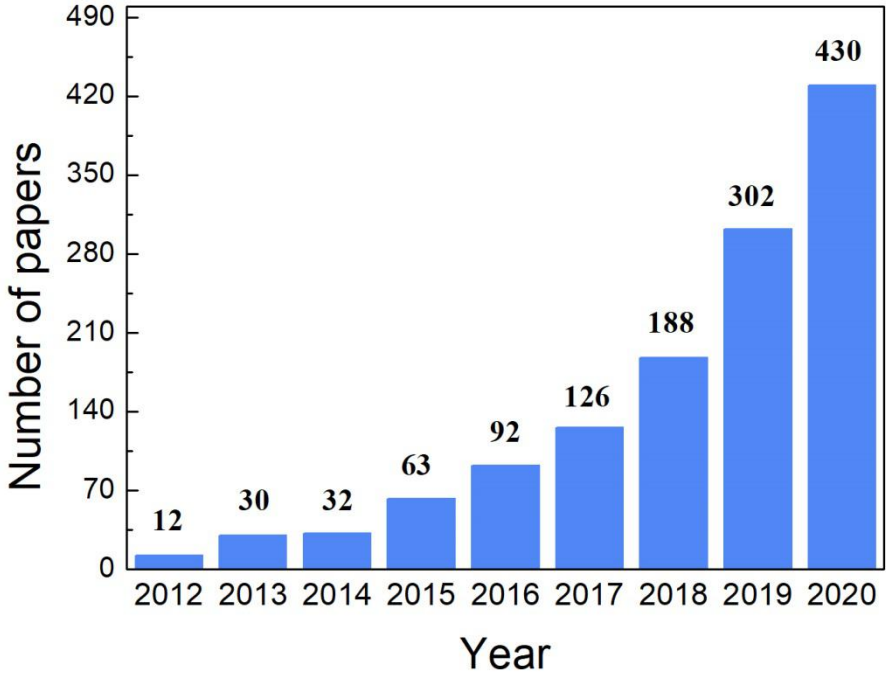

Fig. 1. The number of publications concerning the keywords of "biochar + activation" on indexed journals from 2012 to 2020. The search results are based on the database of "Web of Science".

Fig. 2. The sources of various biochar-based catalysts used in PMS activation and the research gaps between plant-based waste and animal-based waste.

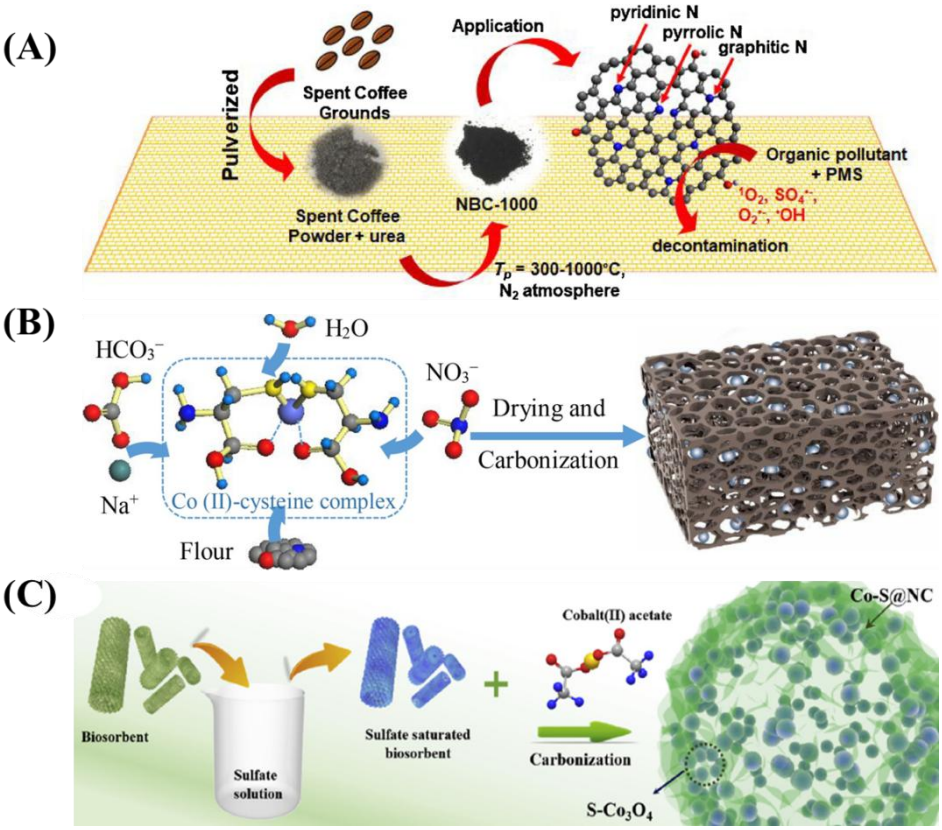

Fig. 3. The synthesis process of (A) Co-N-S-PCs [81], Copyright 2017 Elsevier. (B) NBC [128], Copyright 2018 Elsevier. and (C) Co-S@NC [82]. Copyright 2019 Elsevier.

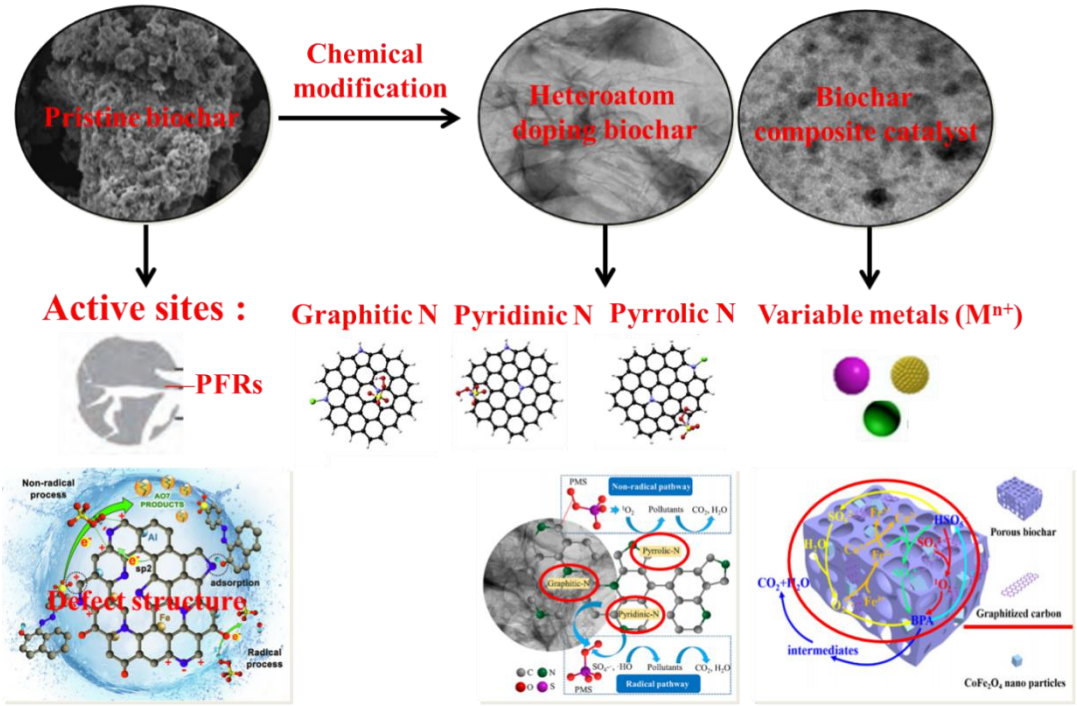

Fig. 4. The biochar-based catalysts used for PMS activation (pristine biochar, heteroatom doping biochar and biochar composites catalysts) and the active sites come from three types of biochar-based catalysts, such as PFRs, graphitization structures and defect structures, N species (graphitic N, pyridinic N and pyrrolic N) and variable metals. Reproduced with permission from Ref. [83, 184, 185]. Copyright 2019 Elsevier.

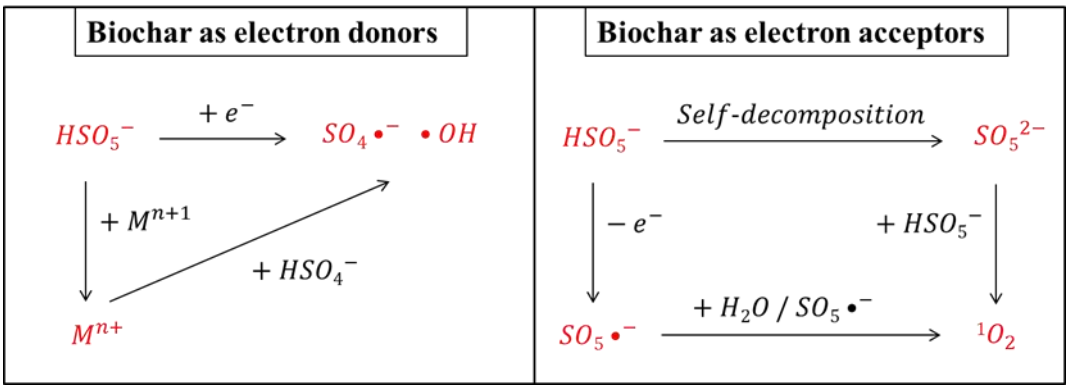

Fig. 5. The generation pathway of $SO_4^{\bullet -}$, •OH and $^1O_2$ and the role of the biochar-based catalysts in the production of ROS.

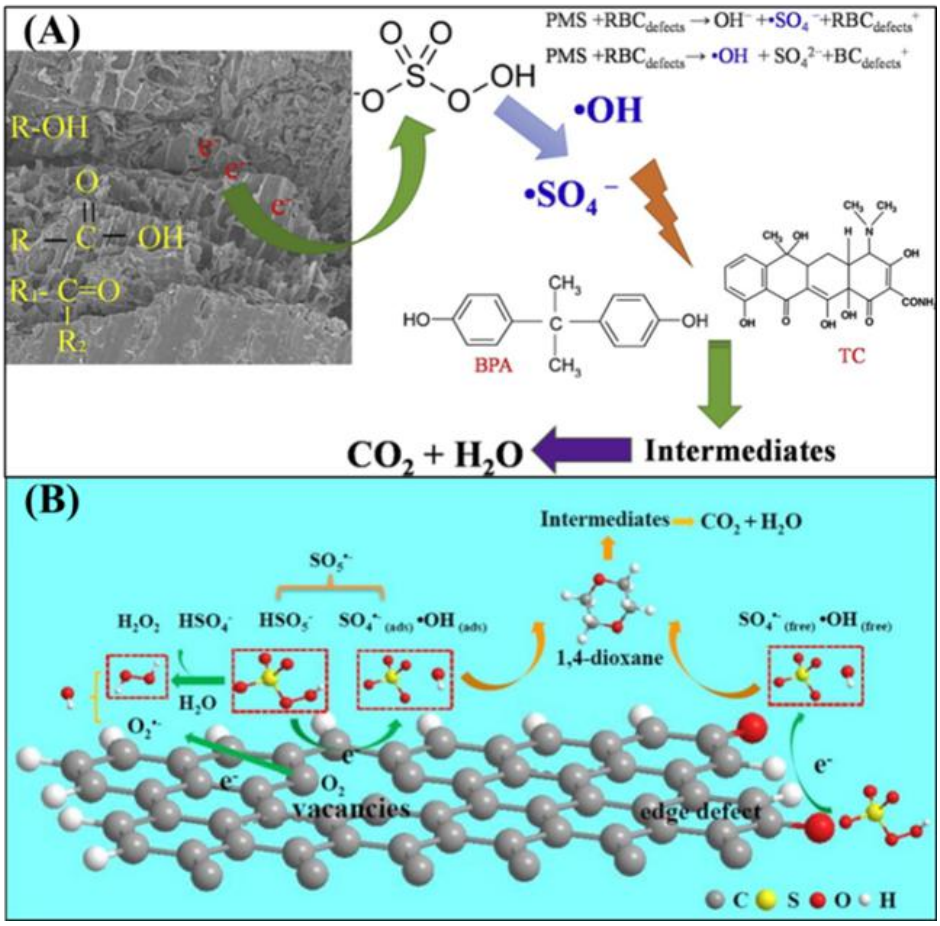

Fig. 6. The intrinsic catalytic mechanism of pristine biochar activating PMS for (A) BPA and TC [97], and (B) 1,4-dioxane degradation [86]. Copyright 2019 Elsevier.

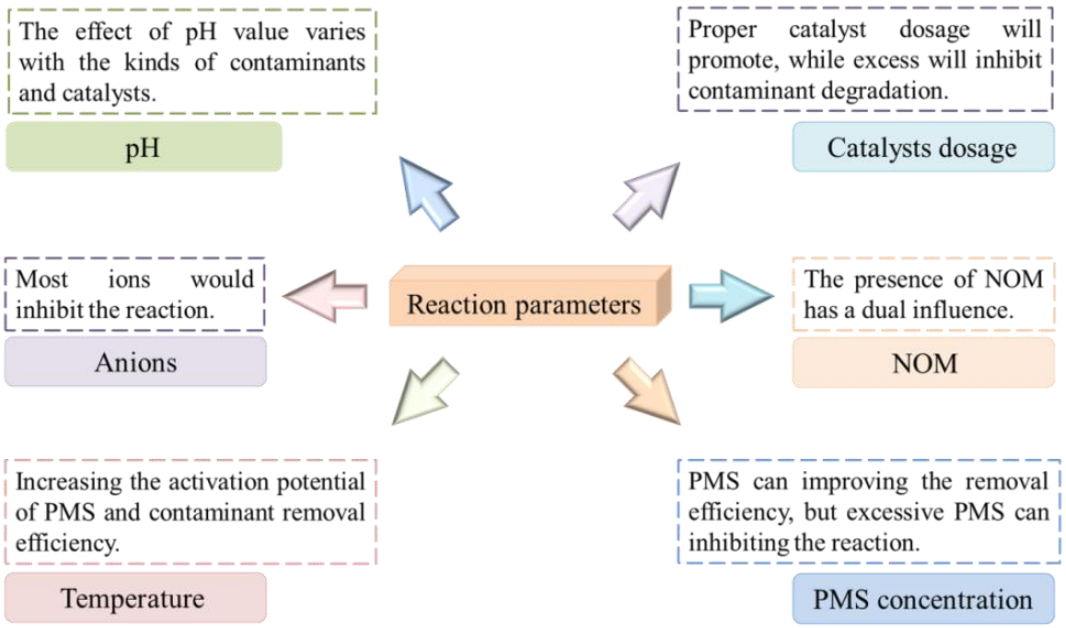

Fig. 7. The influence of various reaction parameters on the biochar/PMS system.

Table .1. Sources and preparations of biochar-based catalysts.

Feedstock	Synthesis method	Process	Product	Ref.
Lignocellulose				
Lignocellulosic waste Old corrugated containers (OCC) $FeCl_3·6H_2O$	Facile solvent-free carbothermal redox approach	20 g OCC and 10 g $FeCl_3·6H_2O$ were first shear mixed. The obtained OCC and $FeCl_3·6H_2O$ mixture was then annealed in a tube furnace at 850 ℃ for 2 h in an N_2 atmosphere with a heating rate of 5 ℃/min.	2D nZVI/biochar (OCF-850)	[54]
Cellulose $Fe(NO_3)_3·9H_2O$ $Co(NO_3)_2·6H_2O$	Pyrolysis	$Fe(NO_3)_3·9H_2O$ (3.2652 g, 8.08 mmol) and $Co(NO_3)_2·6H_2O$ (1.1765 g, 4.04 mmol) were added, and dissolved in 125 mL H_2O. Then the CCNF was added into the above solution. The mixture was then transferred into a Teflon-lined autoclave and heated at 180 ℃ for 24 h.	carbon nanofiber (CCNF) supported cobalt ferrite ($CoFe_2O_4$/CCNF)	[108]
Lignin $CoCl_2$	Pyrolysis	The mixture was placed on a ceramic crucible for pyrolysis in N_2 or CO_2 at a ramping rate of 10 ℃/min to 720 ℃ with a high gas flow rate of 600 mL/min for maintaining the desired atmosphere environment for pyrolysis.	Co-impregnated biochar (CoIB)	[140]
Lignin	Facile one-pot synthesis route	The mixed solution was placed in the Teflon-lined autoclave with a capacity of 100 mL, sealed, and subjected to HTC at 200 ℃ for 18 h. The hydrothermal products were further calcined in a constant flow of N_2 (3 ℃/min) at 550, 700, 800, 900, or 1000 ℃ for 2 h.	Nanoscale zero-valent iron (ZVI) in situ encapsulated in lignin-derived hydrochar (Fe@HC)	[186]
Citrus peels	Pyrolysis	The citrus peels were cut into small strips and then washed with water and ethanol, the clean peels were continuously stirred in ultrapure water for 12 h to separate the TP from the e-TPs. The TP powders were carbonized at different temperatures (350−900 °C) for 90 min in N_2 atmosphere.	Biochar	[64]

Rice straw $Co(NO_3)_2·6H_2O$ $FeSO_4·7H_2O$	Robust impregnation-pyrolysis	2.91 g $Co(NO_3)_2·6H_2O$, 5.56 g $FeSO_4·7H_2O$, urea (3.0 g) and ascorbic acid (2.5 g) were added, then heated to a desired temperature (400–800 ℃) in a muffle furnace with a ramp of 5 ℃/min and maintained for 4 h.	Magnetic nitrogen doped biochar supported $CoFe_2O_4$ composite (MNBC)	[58]
Rice hull $FeSO_4·7H_2O$	Pyrolysis	Dried rice hulls were then loosely placed in a muffle furnace for 6 h at a temperature of 350 ℃ under oxygen-limited condition, nZVI particles were synthesized by reduction of $FeSO_4·7H_2O$ using $NaBH_4$.	Biochar supported nanoscale zero valent iron (BC-nZVI)	[187]
Maize stalk	Pyrolysis	After cut, washed, and dried at 60 ℃ for 24 h, biomass was pyrolyzed in muffle furnace at 300 ℃ for 2 h.	Maize stalk (S)-derived biochars as a carbon-based support for nanoscale zero-valent iron (nZVI).	[188]
Corncob	Pyrolysis	5 g of corncob powder was added to the urea solution in the weight ratio of 1:0, 1:1, 1:2, 1:3 and 1:4, the obtained mixture was transferred to the furnace, heated at 5 ℃/min to 700 ℃ and maintained under a nitrogen flow for 2 h.	N-doped biochars (NBCs)	[189]
Corn stems $Fe(NO_3)_3·9H_2O$ $MnCl_2·4H_2O$	Pyrolysis, one-step strategy and solvothermal method	Pyrolyzed in a tube furnace at 400 ℃ for 3 h with a heating rate of 5 ℃/min in N_2 atmosphere (80 L/min); the solid mixture was grinded, and heated in a tube furnace at 800 ℃ for 2 h with a heating rate of 5 ℃/min in N_2 atmosphere (100 mL/min); the obtained mixture was transferred into a 100 mL Teflon-lined stainless steel autoclave and heated at 180 ℃ for 24 h.	Graphitized hierarchical porous biochar (MX) and $MnFe_2O_4$ magnetic composites ($MnFe_2O_4$/MX)	[148]
Wheat straw $Co(NO_3)_2•6H_2O$	Pyrolysis, modified coprecipitation method	2.0 g of $Co(NO_3)_2·6H_2O$ and 20 g of BC was dissolved in purewater. The resulting precipitate was dried at 70 ℃ for 6 h and calcined in air at 450 ℃ for 4 h.	Biochar (BC)-supported Co_3O_4 composite (Co_3O_4-BC)	[190]

Sawdust $FeCl_3$	Pyrolysis	4.0 g DICY and a certain amount (0, 0.5, 1.0 and 2.0 g) of $FeCl_3$ were first added into 60 mL of pure water. 1 g of sawdust was added into the above mixture and stirred until dry at 80 ℃ in a heated magnetic stirrer. The dry powder obtained was pyrolyzed to form Fe/N co-doped biochar under 800 ℃ for 1 h in a tube furnace under an N_2 atmosphere.	Fe/N co-doped biochar (Fe-N-C)	[191]
Sawdust	Pyrolysis	1.0 g of sawdust and a certain amount (1.0, 2.0, 4.0 and 6.0 g) of the different nitrogen precursors were added to 60 mL of pure water. Then, the resulting mixture was calcined at different thermal annealing temperatures (500, 600, 700 and 800 ℃) under a N_2 atmosphere for 60 min in a tube furnace with the heating rate of 10 ℃/min.	Nitrogen-doped biochar (N-biochar)	[79]
Spent coffee grounds (SCGs)	Facile pyrolysis process	Exactly 400 mg of SCP and 2.0 g of urea were mixed homogeneously in a quartz boat, and then into a horizontal tubular furnace operated under nitrogen atmosphere. The furnace was gradually heated at a heating rate of 10 °C/min to desired T_p and maintained for 1 h.	Redox-active carbocatalyst (NBC)	[128]
Non-lignocellulose				
Sewage sludge (SS)	Urea-mediated pyrolysis	Dried at 60 ℃, grounded into fine particles, and subsequently, transferred into furnace for calcination under 700 ℃ for 2 h (heating rate: 10 ℃/min).	Nitrogen-functionalized sludge carbon (NSC)	[95]
Sludge	Oxygen-limited pyrolysis	Dried coagulation sludge was grinded and sifted through 100 mesh sieve. 10 g sludge was calcined at 400, 500, 600 and 700 ℃ for 2 h under argon atmosphere, respectively.	Biochar	[192]
Sludge	Pyrolysis	Dried sewage sludge was pyrolysis to form SDBC under 700 ℃ for 2 h in a tubular furnace under a N_2 flow with the temperature increasing at a rate of 10 ℃/min.	Sludge-derived biochar (SDBC)	[193]

Sludge	Facile one-step pyrolysis	Dried sludge was mixed with urea at a mass ratio (urea/dried sludge) of 2/1. The mixture was fully grinded and calcined at 500, 600, 700, or 800 ℃ under N_2 atmosphere (100 mL/min) for 120 min in a tubular furnace (OTF-1200X, Hefei, China) with a ramping rate of 10 ℃/min.	Nitrogen-doped carbon (NC)	[168]
Yeast cells	One-step calcination procedure	The powder mixture was calcined at 700 ℃ for 2 h with ramping rate of 5 ℃/min. The annealed samples were washed with distilled water to remove the salts and then dried in a vacuum oven at 60 ℃ overnight.	Nitrogen-doped biochar nanosheets (NCS-x)	[185]
Food waste digestate	Pyrolysis	500 g of the dry food waste digestate was fed into the chamber of an atmosphere furnace. Nitrogen flow of 3 L/min was pumped in the furnace for about 10 min to ensure an oxygen-free atmosphere. Then, the N_2 flow was decreased to 0.2 L/min, and the furnace was heated to 800 ℃ with a heating rate of 5 ℃/min. The temperature was hold for 100 min.	Food waste digestate biochar (FWDB)	[60]
Human hair	Pyrolysis	12.0 g of human hair was mixed with 100 mL of KOH solution (1.13 M), pyrolysis at a predetermined temperature (700, 800, and 900 ℃) for 1 h with a heating rate of 2 ℃/min under N_2 atmosphere.	Nitrogen and sulfur codoped carbon (NSC)	[59]

Table. 2. The performances of biochar catalysts as PMS activator for the degradation of various organic contaminants.

Pollutants	Catalysts	Optimal experiment terms	Removal rate	Ref.
Pharmaceuticals				
Triclosan (TCS)	Sludge-derived biochar (SBC)	pH 7.2, SBC dosage of 1.0 g/L and PMS concentration of 0.8 mM at 25 °C.	99.2%	[88]
Sulfapyridine (SPY)	Biochar-supported Fe composite (Fe/C)	[SPY] = 10 mg/L, [PMS] = 1 mM, [catalyst] = 0.5 g/L, pH = 8.2.	100%	[194]
Chloramphenicols	Biochar (BC)-supported Co_3O_4 composite (Co_3O_4-BC)	10 wt% Co_3O_4 loading on BC, 0.2 g/L Co_3O_4-BC, 10 mM PMS and pH = 7	Almost 100% (10min)	[190]
sulfamethoxazole (SMX)	Co_9S_8 and CoO encapsulated by nitrogen and sulfur co-doped sludge-derived biochar (CoO/Co_9S_8@N-S-BC)	$[PMS]_0$ = 1.6 mM, $[SMX]_0$ = 0.08 mM, [Catalyst] = 0.2 g/L, pH = 3.0, T = 25 ℃.	100% (20min)	[134]
Acetaminophen (ACE)	Co-impregnated biochar (CoIB)	Catalyst = 50 mg/L, ACE = 5 mg/L, PMS = 200 mg/L, and T = 30 ℃.	>90%	[140]
Ofloxacin (OFX)	Co_3O_4 fabricated with assistance of rice straw derived biochar (BC-Co_3O_4)	[OFX] = 50 μM, [Oxone] = 0.5 mM, [BC-Co_3O_4] = 0.2 g/L, pH = 7, T = 25 ℃	>90% (10 min)	[46]
Tetracycline (TC)	Rice husk biochar (RBC)	pH 6.0, 0.2 g RBC, PMS concentration of 20 mM, 20 mg/L TC.	90.3%	[97]
Tetracycline (TC)	Nitrogen-doped biochar fiber (PGBF-N)	[biochar fiber] = 0.1 g/L, [PMS] = 1 mM, [temperature] = 25 ℃, [TC] = 20 mg/L.	100%	[144]
Tetracycline (TC)	Cobalt-impregnated biochar (Co-SCG)	TC concentration of 0.2 mM, PMS concentration of 0.6 mM, Co-SCG dosage of 100 mg/L, and pH of 7.0.	97%	[161]

Organic dyes				
Rhodamine B (RhB)	Biochar (BC)	PMS dosage = 30 mg/L, initial RhB concentration = 10 mg/L, catalyst dosage = 0.5 g/L.	81.9%	[192]
Methylene blue (MB)	Nitrogen-doped carbon (NC)	$[MB]_0$ = 50 mg/L, catalyst = 0.3 g/L, PMS = 0.2 g/L and temperature = 25 ℃.	98.7%	[168]
Acid orange 7 (AO7)	N-doped biochar	[catalyst] = 0.1 g/L, pollutant: PMS ratio = 1:50, pH = 3-4 and [AO7] = 10 mg/L.	100% (30min)	[78]
Acid orange 7 (AO7)	A sludge derived carbon-supported MnO_x (ASMn-Nb)	Catalysts = 0.2 g/L, AO7 = 20 mg/L, PMS = 1.6 mM, pH=10, T=25 ℃.	100%	[150]
Acid Orange 7 (AO7) Methylene Blue (MB)	Biochar supported copper oxide composite (BC-CuO)	$[Na_2SO_4]$ = 200 mM, [PMS] = 2 mM, [catalyst] = 0.2 g/L, [MB] = 0.1 mM, [Acid orange7 (AO7)] = 0.1 mM, initial pH= 7.	100% 99.68%	[195]
Orange II	Graphitized hierarchical porous biochar (MX) and $MnFe_2O_4$ magnetic composites ($MnFe_2O_4$/MX)	$[PMS]_0$ = 0.5 g/L, $[Catalyst]_0$ = 0.05 g/L, $[MnFe_2O_4/MS]_0$ = 0.05 g/L, $[orange\ II]_0$ = 20 mg/L, initial pH = 5.8, T = 25 ℃.	92% ($MnFe_2O_4$/ML) 95% ($MnFe_2O_4$/MC)	[148]
Endocrine disruptors				
Bisphenol A (BPA)	Biochar (BC)	pH 6.0, 0.2 g/L catalyst, 0.1 g/L PMS, and 10 ppm initial BPA in 0.1 M phosphate buffer.	~80% (TOC)	[153]
Bisphenol A (BPA)	N-doped biomass-derived carbon (NBC)	[BPA] = 5 mg/L, [Oxone®] = 0.30 g/L, [catalyst] = 0.20 g/L, reaction time = 60 min, and pH = 4.0.	99 ± 1% (NBC-1000)	[128]
Bisphenol A (BPA)	N-doped porous carbons (N-doped PCs)	[BPA] = 5 mg/L, [catalyst] = 0.20 g/L, [PMS] = 0.30 g/L, and pH = 4.0.	>95% (PC-SC)	[62]

Bisphenol A (BPA)	Nitrogen-doped biochar (N-biochar)	BPA = 10 mg/L, initial pH = 6.28, catalyst concentration = 0.5 g/L, PMS concentration = 2.0 mM, temperature = 25 ℃.	100% (5min)	[79]
Bisphenol A (BPA)	Biochar loaded with $CoFe_2O_4$ nanoparticles ($CoFe_2O_4$/HPC)	$[PMS]_0$ = 0.5 g/L, $[CoFe_2O_4/HPC]_0$ = 0.05 g/L, $[BPA]_0$ = 10 mg/L, initial pH = 7.4, T = 25 ℃.	100% (8min)	[83]
Bisphenol A (BPA)	Nitrogen-doped biochar nanosheets (NCS-x)	Catalyst = 0.4 g/L, PMS =0.4 g/L, BPA = 20 mg/L, temperature = 25 ℃ and pH = 7.	100% (6min, NCS-6)	[185]
Bisphenol A (BPA)	Nitrogen and sulfur codoped carbon (NSC)	[NSC-X] = 0.08 g/L, [Oxone] = 0.40 g/L, and [BPA] = 25 mg/L.	96.4% (NSC-900)	[59]
Biphenol A (BPA)	Iron embedded carbon composites (Fe-BC-700)	100 mL solution, 20 mg/L BPA, 0.2 g/L PMS and 0.15 g/L catalyst.	100% (5 min)	[101]
Pesticides				
Dinotefuran (DIN)	S-Co_3O_4 in nitrogen doped carbon martix (Co-S@NC)	Catalyst dose = 0.1 g/L, $[DIN]_0$ = 10 mg/L, $[PMS]_0$ = 0.65 mM, pH = 4.8	100%	[82]
Metolachlor (MET)	Magnetic nitrogen doped biochar-supported $CoFe_2O_4$ composite (MNBC)	[MET] = 10 mg/L, [Catalyst] = 200 mg/L, [PMS] = 0.5 mM, [Reaction time] = 40 min, pH unadjusted.	100% (MNBC-800)	[58]
Others				
p-hydroxybenzoic acid (HBA)	Core-shell Co@C nanoparticles with nitrogen and sulfur into hierarchically porous carbons (Co-N-S-PCs).	Catalyst = 0.066 g/L, PMS = 6.5 mM, T = 25 ℃.	>98%	[81]
p-hydroxybenzoic acid (HBA)	Fe_3O_4 and porous biochar composites (Fe_3O_4/MC)	$[PMS]_0$ = 1.0 g/L, $[catalyst]_0$ = 0.2 g/L, $[HBA]_0$ = 10 mg/L, T = 25 ℃.	Almost 100% (Fe_3O_4/MC700)	[147]

Trichloroethylene (TCE)	Biochar-based support for nanoscale zero-valent iron (Fe-CB600)	TCE concentration: 0.1 mM, catalyst dosage: 1 g/L, PMS concentration: 5 mM, pH = 8.2, T = 25 ℃.	100% (Fe-CB600, 20 min)	[188]
Phenol	Nanoscale zero-valent iron (ZVI) in situ encapsulated in lignin-derived hydrochar (Fe@HC)	20 ppm phenol; 2 g/L PMS; 0.4 g/L catalyst; 30 ℃; without pH adjustment	100% (20min)	[186]
1,4-dioxane	Biochar (BC)	[PMS] = 8.0 mM, [1,4-dioxane] = 20.0 μM, [biochar] = 1.0 g/L, [DMPO] = 100.0 mM ((c)), [Temperature] = 25 ℃ and the initial pH was 6.5.	84.2% (BC-800)	[86]